

Specialization of Hepatitis C Virus Envelope Glycoproteins for B Lymphocytes in Chronically Infected Patients

Florian Douam,^{a,b,c,d,e,f,g*} Louis-Marie Bobay,^{h*} Guillemette Maurin,^{a,b,c,d,e} Judith Fresquet,^{a,b,c,d,e} Noémie Calland,^{a,b,c,d,e} Carine Maise,ⁱ Tony Durand,^j François-Loïc Cosset,^{a,b,c,d,e,f} Cyrille Féray,^k Dimitri Lavillette^{a,b,c,d,e,g*}

CIRI, International Center for Infectiology Research, Team EVIR, Université de Lyon, Lyon, France^a; INSERM, U1111, Lyon, France^b; Ecole Normale Supérieure de Lyon, Lyon, France^c; Université Claude Bernard Lyon 1, Centre International de Recherche en Infectiologie, Lyon, France^d; CNRS, UMR5308, Lyon, France^e; LabEx Ecofect, Université de Lyon, Lyon, France^f; CNRS, UMR 5557 Microbial Ecology, Microbial Dynamics and Viral Transmission Team; Université Claude Bernard Lyon 1, Université de Lyon, Lyon, France^g; CNRS, UMR3525, Microbial Evolutionary Genomics, Institut Pasteur, Université Pierre et Marie Curie, Cellule Pasteur UPMC, Paris, France^h; INRA, UMR754, ENVL, Rétrovirus et Pathologie Comparée, Université Claude Bernard Lyon 1, Université de Lyon, Lyon, Franceⁱ; UMR913, Institut des Maladies de l'Appareil Digestif (IMAD), Faculté de Médecine, INSERM, Nantes, France^j; INSERM, U955, Groupe Hospitalier Universitaire Albert Chenevier-Henri Mondor, Créteil, France^k

ABSTRACT

Hepatitis C virus (HCV) productively infects hepatocytes. Virion surface glycoproteins E1 and E2 play a major role in this restricted cell tropism by mediating virus entry into particular cell types. However, several pieces of evidence have suggested the ability of patient-derived HCV particles to infect peripheral blood mononuclear cells. The viral determinants and mechanisms mediating such events remain poorly understood. Here, we aimed at isolating viral determinants of HCV entry into B lymphocytes. For this purpose, we constructed a library of full E1E2 sequences isolated from serum and B lymphocytes of four chronically infected patients. We observed a strong phylogenetic compartmentalization of E1E2 sequences isolated from B lymphocytes in one patient, indicating that E1E2 glycoproteins can represent important mediators of the strong segregation of two specialized populations in some patients. Most of the E1E2 envelope glycoproteins were functional and allowed transduction of hepatocyte cell lines using HCV-derived pseudoparticles. Strikingly, introduction of envelope glycoproteins isolated from B lymphocytes into the HCV JFH-1 replicating virus switched the entry tropism of this nonlymphotropic virus from hepatotropism to lymphotropism. Significant detection of viral RNA and viral proteins within B cells was restricted to infections with JFH-1 harboring E1E2 from lymphocytes and depended on an endocytic, pH-dependent entry pathway. Here, we achieved for the first time the isolation of HCV viral proteins carrying entry-related lymphotropism determinants. The identification of genetic determinants within E1E2 represents a first step for a better understanding of the complex relationship between HCV infection, viral persistence, and extrahepatic disorders.

IMPORTANCE

Hepatitis C virus (HCV) mainly replicates within the liver. However, it has been shown that patient-derived HCV particles can slightly infect lymphocytes *in vitro* and *in vivo*, highlighting the existence of lymphotropism determinants within HCV viral proteins. We isolated HCV envelope glycoproteins from patient B lymphocytes that conferred to a nonlymphotropic HCV the ability to enter B cells, thus providing a platform for characterization of HCV entry into lymphocytes. This unusual tropism was accompanied by a loss of entry function into hepatocytes, suggesting that HCV lymphotropic variants likely constitute a distinct but parallel source for viral persistence and immune escape within chronically infected patients. Moreover, the level of genetic divergence of B-cell-derived envelopes correlated with their degree of lymphotropism, underlining a long-term specialization of some viral populations for B-lymphocytes. Consequently, the clearance of both hepatotropic and nonhepatotropic HCV populations may be important for effective treatment of chronically infected patients.

Hepatitis C virus (HCV) infection is a major health concern, with more than 170 million infected people worldwide. Chronically infected patients may develop cirrhosis, liver failure, or hepatocellular carcinoma (1), but also extrahepatic disorders, including mixed cryoglobulinemia (2, 3), B-cell non-Hodgkin's lymphomas, or autoimmune diseases (3, 4). Whether the pathophysiologic scenarios leading to such disorders involve a chronic and sustained stimulation of the immune system or, in contrast, direct infection and transformation of lymphoid cells is still a matter of debate.

HCV E1 and E2 envelope glycoproteins play a major role in HCV entry (5), allowing viral attachment of the viral particle to several receptors, endocytosis, and fusion of the viral membrane with the endosomal membrane. Several cellular receptors have been identified so far. The tetraspanin CD81 (6) is ubiquitously expressed and is found in B lymphocytes, where it acts as a co-

Received 1 October 2015 Accepted 27 October 2015

Accepted manuscript posted online 4 November 2015

Citation Douam F, Bobay L-M, Maurin G, Fresquet J, Calland N, Maise C, Durand T, Cosset F-L, Féray C, Lavillette D. 2016. Specialization of hepatitis C virus envelope glycoproteins for B-lymphocytes in chronically infected patients. *J Virol* 90:992–1008. doi:10.1128/JVI.02516-15.

Editor: M. S. Diamond

Address correspondence to Dimitri Lavillette, dimitri.lavillette@univ-lyon1.fr.

* Present address: Florian Douam, Department of Molecular Biology, Princeton University, Princeton, New Jersey, USA; Louis-Marie Bobay, Department of Integrative Biology, University of Texas at Austin, Austin, Texas, USA; Dimitri Lavillette, Institut Pasteur Shanghai, Chinese Academy of Sciences, SIBS Campus, Shanghai, China. F.D. and L.-M.B. contributed equally to this article.

Copyright © 2015, American Society for Microbiology. All Rights Reserved.

stimulatory molecule. However, other entry factors such as the scavenger receptor BI (SR-BI) (7) and the tight junction proteins claudin-1 (CLDN1) (8) and occludin (9) have more restricted expression profiles. The combination of receptors and expression rates in hepatocytes is one element that explains why the liver constitutes the main target for HCV particles. However, many studies have shown that HCV may also infect peripheral blood mononuclear cells (PBMCs) (10–17). Indeed, the presence of positive or negative HCV RNA as well as structural or nonstructural viral proteins has been characterized in PBMCs of chronically HCV-infected patients or in perihepatic lymph nodes (12–16, 18). Other studies have reported the ability of serum-derived HCV particles to infect PBMCs (3, 4) or particular human T-cell leukemia virus type 1-infected cell lines (19, 20). More recently, a lymphocyte-derived CD5 molecule was identified as essential for infection of T cells with native patient-derived HCV (21). Finally, a study reported the establishment of a B-cell line deriving from a HCV-infected patient non-Hodgkin's B-cell lymphoma (22). This B-cell line was able to replicate and produce a particular "SB" full-length HCV variant which was able to infect hepatocytes but also PBMCs and B-lymphocyte cell lines (22). However, no viral propagation in these newly infected cell lines has been robustly demonstrated so far.

Interestingly, HCV lymphotropism is also highly supported by the presence of a nonrandom phylogenetic distribution between HCV quasispecies deriving from PBMCs and serum compartment (12, 13, 18, 23). This phenomenon, called compartmentalization, suggests a specialization of particular HCV variants to lymphocyte infection. So far, this compartmentalization has been reported for the internal ribosome entry site (IRES) sequences (12, 13, 18) or for the short hypervariable region 1 (HVR1) of envelope glycoprotein E2 in the setting of chronic infection (17) or liver transplantation (23). Only one study demonstrated the specialization of the IRES-derived lymphotropic quasispecies *in vitro* by reporting a difference in translational efficiency of IRES between hepatocyte and extrahepatic sequences (12). However, it is impossible to study other aspects of lymphotropic infection as JFH-1 cell-culture-produced HCV (HCVcc) cannot infect and replicate in PBMC types (24, 25).

To better approach the paradox between the observed *in vivo* and *in vitro* tropism and to identify lymphotropism determinants in viral proteins, we combined for the first time phylogenetic compartmentalization analysis of full-length E1E2 sequences from chronically infected patients with functional studies using *in vitro* infection assays. We collected serum and B-cell samples from 13 chronically infected patients and managed to construct a substantial collection of complete E1E2 sequences deriving from serum and B cells for four chronically infected patients. We showed that one patient harbored a high divergence rate and a clear phylogenetic dichotomy between lymphocyte- and serum-derived glycoproteins. Strikingly, this dichotomy was correlated to the ability of lymphocyte-derived E1E2 sequences to confer to viral particles the ability to enter into different lymphocyte cell lines. By incorporating two lymphocyte-derived envelope glycoproteins onto the JFH-1 virus, we were able to convert the entry tropism of this virus from hepatotropism to lymphotropism.

Thus, our results suggest that some E1E2 genetic determinants are involved in the maintenance and the strong lymphocyte specialization of a distinct viral subpopulation and provide an interesting tool for further characterization of virus entry within B

lymphocytes. The characterization of such viral variants as well as of their genetic basis represents an important step toward a better understanding of HCV extrahepatic pathogenesis, virus persistence, and immune escape.

MATERIALS AND METHODS

Patients. Serum and B lymphocytes (CD19) were isolated from 13 patients chronically infected by HCV. Patients did not receive any treatment before sample collection, and they did not present any sign of lymphomas.

Cell lines and reagents. Human Huh-7.5 cells (a kind gift from C. Rice, Rockefeller University, NY) and 293T kidney cells (ATCC CRL-1573) were grown in Dulbecco's modified Eagle's medium (DMEM) (Invitrogen) supplemented with 10% fetal bovine serum (FBS). Raji (ATCC CCL-86), Daudi (ATCC CCL-213), Molt4 (ATCC CRL-1582), and X174 (ATCC CRL-1951) cells were grown in RPMI 1640 medium (Invitrogen) supplemented with 10% fetal bovine serum (FBS). For Western blotting, the rat anti-E2 clone 3/11 (26) and the mouse anti-HCV E2 clone H52 (27) are kind gifts from J. Dubuisson (Institut Pasteur, Lille, France) and H. Greenberg (Stanford University, CA), respectively. Murine leukemia virus (MLV) capsid was detected by a goat anti-MLV-CA antibody anti-p30 (Viomed). CD81 staining and neutralization assays were performed using the mouse anti-human CD81 JS81 clone conjugated with R-phycoerythrin (BD Biosciences). NS5A-positive cells and HCVcc focus-forming units (FFU) were determined after immunostaining with a mouse anti-HCV NS5A antibody 9E10 (28) (kind gift of C. Rice).

RNA isolation and E1E2 cloning. Viral RNAs were isolated from serum using the QIAamp viral RNA minikit (Qiagen) or from B lymphocytes (CD19) and Raji cell lines using the RNeasy minikit (Qiagen). E1E2 envelope glycoprotein sequences were reverse transcribed (Superscript II; Invitrogen), amplified through two successive nested PCRs, and cloned into a pCMV expression plasmid in fusion with the C-terminal part (18 amino acids) of the HCV core (H77; GenBank accession no. AF009606) encoding sequence that acts as a signal peptide sequence.

Production of HCVpp and infection. HCV pseudoparticles (HCVpp) were produced in 293T cells and used to infect cell lines as previously described (29, 30). Infected cells were quantified by FACSCanto II (BD Biosciences) to measure percentages of green fluorescent protein (GFP) expression. Prior to infections, equivalent levels of MVLC-CA in cell supernatant for each HCVpp were verified in order to ensure infection with equal amounts of pseudoparticles.

Expression and incorporation of E1E2 glycoproteins into viral particles. Transfected 293T cells were lysed, and the nucleus was removed by centrifugation at 12,000 rpm for 10 min. Pseudoparticles were purified and concentrated from the cell culture medium by ultracentrifugation at $82,000 \times g$ for 1 h 45 min through a 20% sucrose cushion. Cell lysates and viral pellets were subjected to Western blot analysis using antibody 3/11 and an anti-MLV-CA antibody as described previously (29).

HCVcc production, infection, and quantification. Plasmid pFK H77/JFH1/HQL (a kind gift of R. Bartenschlager), displaying adaptive mutations (Y835H in NS2, K1402Q in NS3, and V2440L in NS5A) that enhance the production and infectivity of HCVcc particles, was used. L1a and L3k E1E2-encoding sequences (without core-encoding sequences) were inserted into the H77/JFH1/HQL genome to generate, respectively, the L1a/JFH1 and L3k/JFH1 recombinant genomes. Derived HCV RNAs were electroporated in Huh-7.5 cells as described previously (7, 29). Huh-7.5 cells were infected with different dilutions of cell culture supernatants harvested at 48 h and 72 h postelectroporation or with intracellular viral particles obtained 72 h postelectroporation after 3 freeze-thaw cycles of Huh-7.5. Four days postinfection, focus-forming units (FFU) were visualized after NS5A immunostaining. To quantify viral particle production, viral RNAs were isolated from cell supernatant using Tri Reagent solution (Sigma-Aldrich) as recommended by the manufacturer. Viral RNAs were then reverse transcribed using random primers (Bio-Rad) and quantified by quantitative PCR (qPCR) using a light cycler LC480 (Roche Applied Science) as described previously (29).

Raji cell infections. For HCVcc infection of Raji cells, Huh7.5 cells were electroporated with different HCVcc viruses, and cell culture supernatants were collected 72 h postelectroporation. Viral RNAs were isolated from cell supernatant using Tri Reagent solution (Sigma-Aldrich) as recommended by the manufacturer, reverse transcribed using random primers (Bio-Rad), and quantified by qPCR as described previously (29) using JFH-1-specific primers. Following reverse transcription qPCR (RT-qPCR), 5×10^5 Raji cells were then infected with equal amount of genome equivalent (GE) viral particles (4.5×10^5 genome-equivalent viral particles). Infection was stopped 4 days postinfection. Cells were fixed with 2% formaldehyde for 20 min at room temperature and then washed and permeabilized with Perm/Wash buffer (BD Biosciences) for 15 min at 4°C. NS5A expression levels were then quantified using anti-NS5A antibody 9E10 by flow cytometry (FACSCanto II; BD Biosciences). To quantify viral particle production, Raji cell supernatants were collected 4 days postinfection. Viral RNA was isolated using Tri Reagent solution (Sigma-Aldrich), reverse transcribed using random primers (Bio-Rad), and quantified by qPCR as described previously. In parallel, Raji cells were harvested 4 days postinfection, washed and lysed (RNeasy minikit; Qiagen). Total cell-associated viral RNAs were then isolated using the RNeasy minikit (Qiagen). To quantify viral RNA within Raji cells, total RNA was either subjected to 2 rounds of nested PCR using JFH-1- and E1E2-specific primers successively or to a one-step reverse transcription-PCR (RT-PCR). One-step RT-PCR was performed using Multicode-RTx HCV RNA kit (Eragen; for HCV RNA quantification) or a one-step RT-qPCR SYBR green kit (Bio-Rad; for GAPDH [glyceraldehyde-3-phosphate dehydrogenase] mRNA quantification) and a light cycler LC480 (Roche Applied Science), according to the manufacturers' instructions.

Anti-CD81 and bafilomycin A1 neutralization assays. For the CD81 neutralization assay, 5×10^5 Raji cells were incubated with anti-human CD81 antibody (JS81 clone R-phycoerythrin conjugated at a dilution of 1/100; BD Biosciences) for 1 h at 37°C. Cells were then washed with phosphate-buffered saline (PBS) two times and infected with equivalent amount of HCVcc particles as described above. For the bafilomycin A1 neutralization assay, Raji cells were pretreated with dimethyl sulfoxide (DMSO) or 20 nM bafilomycin A1 for 30 min at 37°C. Cells were infected with equivalent amount of different HCVcc viruses premixed with DMSO or 20 nM bafilomycin A1. Four days postinfection, cells were lysed (RNeasy minikit; Qiagen), total RNA was extracted, and the levels of cell-associated viral RNA and GAPDH mRNA were determined by one-step RT-qPCR as described above. To control the absence of toxicity of the bafilomycin A1 on cell viability and surface protein expression, naive Raji cells were pretreated for 30 min with DMSO or 20 nM bafilomycin A1, washed, and then incubated for 4 days with cell medium premixed with DMSO or with 20 nM bafilomycin A1, respectively. Cells were then stained using a propidium iodide staining solution (Affymetrix) and an anti-CD81 antibody (JS81 clone R-phycoerythrin conjugated at a dilution of 1/100; BD Biosciences) for 15 min and 1 h, respectively, at 4°C, washed two times, and fixed (1% paraformaldehyde [PFA], 1% FBS, PBS). Cell population profiles, cell death, and CD81 expression were then assessed by flow cytometry (FACSCanto II; BD Biosciences). For the vesicular stomatitis virus pseudoparticle (VSVpp) entry inhibition assay, Raji cells were treated with DMSO and 10, 25, or 50 nM bafilomycin A1 for 30 min at 37°C. Cells were then washed two times and infected with equivalent amount of VSV glycoprotein-harboring pseudoparticles (VSVGpp) premixed with DMSO or with the respective bafilomycin A1 concentration. Six hours postinfection, cells were washed with PBS two times and incubated at 37°C. Four days postinfection, cells were fixed (1% PFA, 1% FBS, PBS), and GFP expression was analyzed by flow cytometry (FACSCanto II; BD Biosciences).

Individual and global phylogenetic analysis. E1E2 sequences were translated into protein sequences and aligned with MUSCLE v3.6 (31) for each patient individually or altogether. For individual analysis, reference sequences of genotypes 1b (gt1b) (AY734975), 2a (AY734977), and 3a (AY734984) were included for patients 1, 2, and 3, respectively. For global

analysis, reference sequences of genotypes 1b, 2a, and 2b (AAW65874) as well as 3a were included. The E1E2 sequence of virus SB was also added. Sequence S2g was removed from the protein alignment as several insertions and/or deletions led to an aberrant protein sequence when aligned. Misaligned regions were removed with BMGE (32). A maximum likelihood tree was built under the LG + G model (4) with PhyML v3.0.1 (33). Then 100 bootstrap replicates were generated with the same model to assess the tree topology. The tree was rooted using the midpoint root. A tree based on the nucleotide alignment of the same data set (but including S2g) was built with the same methods and programs under a GTR + G model (4) and gave a consistent topology.

Statistical analysis. Statistical analyses were performed using a Mann-Whitney or Wilcoxon test. When applicable, data are presented as mean \pm standard deviation and results of the statistical analysis are shown as follows: ns, nonsignificant ($P > 0.05$); *, significant ($P < 0.05$); **, very significant ($P < 0.01$).

Nucleotide sequence accession numbers. Nucleotide sequences have been submitted to GenBank under the following accession numbers: H77 gt1a envelope, AF009606; SB complete genome, KM349851.1; JFH-1 genome, AB047639; J6 gt2a envelope, AF177036; UKN3A envelope, AY734985; Ref1b envelope, AY734975; Ref2a envelope, AY734977; Ref2b envelope, AAW65874; and Ref3a envelope, AY734984.

RESULTS

Construction of an E1E2 collection from patient's sera and B lymphocytes. To analyze E1E2 compartmentalization and identify potential lymphotropic sequences, we first aimed at generating a collection of E1E2 sequences collected from both serum and B cells of 13 chronically infected patients. Using a limited dilution protocol (34), we successfully managed to isolate and amplify, by reverse transcription and nested PCR, 119 E1E2 sequences from sera and B lymphocytes of nine patients (Fig. 1). All of the isolated cDNA was then cloned into the expression plasmid and sequenced. To limit the risk of a genetic bottleneck due to cDNA amplification from a single pool of isolated viral RNA, we performed several cDNA amplifications from independent viral RNA preparations, derived from both patient compartments (serum and B cells).

Despite different strategies, no sequence amplification could be achieved in 4 patients. For four other patients, the amount of E1E2 sequences isolated per patient (22 in total) was not sufficient for further phylogenetic analysis. Indeed, for these patients, only serum-derived sequences (6 sequences from 2 patients) or a limited number of both serum- and B-cell-derived sequences (16 sequences from 2 patients) could have been isolated (Fig. 1).

In contrast, the numbers of E1E2 sequences isolated per patient were substantial in both compartments for the five remaining patients (97 sequences in total: 52 serum-derived sequences and 45 B-cell-derived sequences) (Fig. 1). However, as E1E2 sequences harbored a significant genetic diversity for only four patients, we decided to use the sequences deriving from these patients' serum and B-cell compartments for our phylogenetic and functional studies (Fig. 1). In total, 80 sequences were isolated from these patients, of which 42 were serum derived and 38 were B-cell derived. These four patients, designated patients 1, 2, 3, and 4, harbored serum-derived sequences of genotypes 1b (gt1b), 2a, 3a, and 2b, respectively (Fig. 1).

E1E2 sequences present a strict compartmentalization in some chronically infected patients. We then aimed to analyze the phylogenetic compartmentalization of our collection of E1E2 sequences for each patient individually. The trees obtained for patients 2, 3, and 4 display no clear separation between serum-de-

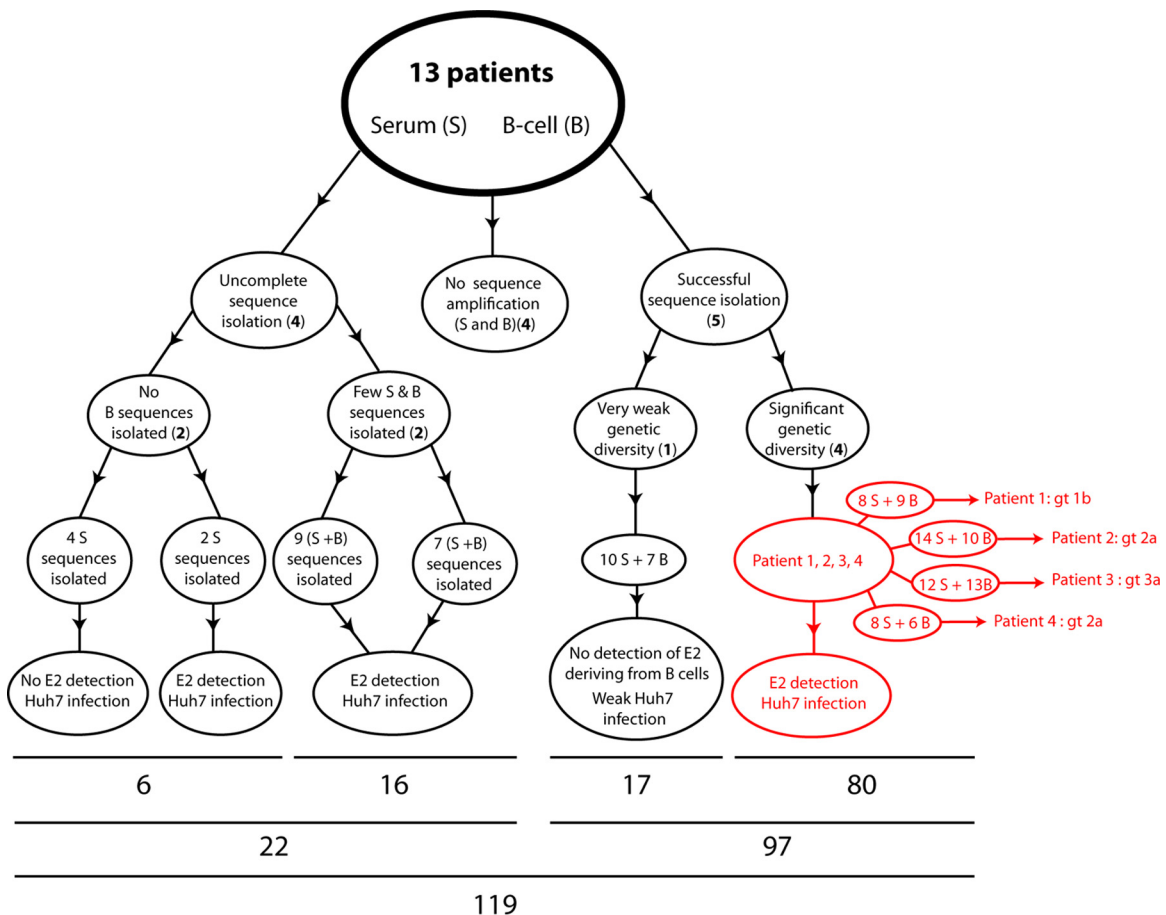


FIG 1 Summary of the experimental procedures leading to the construction of a collection of E1E2 sequences deriving from serum and B cells of different chronically infected patient. Serum (S) and B-cell (B) samples from 13 chronically infected patients were used to isolate and construct a collection of patient-derived E1E2 sequences. Arrows indicate the different experimental routes engaged during the construction of the E1E2 collection (from top to the bottom). The two first rows of circles indicate the different experimental outcomes encountered during sequence isolation and amplification in this study. Boldface numbers in parentheses indicate the number of patients for each experimental procedure outcome. The third row of circles indicates the precise number of sequences isolated for each sequence isolation experimental outcome. The last row of circles resume basic functional analysis performed for each sequence isolation experimental outcome. “E2 detection” indicates that expression of E2 in HEK293T cells was detected for at least one isolated E1E2 sequence; “Huh7 infection” indicates that a significant infection of Huh-7 was detected for at least one isolated E1E2 sequence incorporated onto a pseudoparticle. Numbers located below the schematic representation indicate the number of isolated sequences in total or per group of sequence isolation experimental outcome. The collection of E1E2 sequences used for further phylogenetic and functional analysis in this study is highlighted in red. S, serum-derived sequences; B, B-cell-derived sequences.

rived (named S2, S3, and S4) and lymphocyte-derived (named L2, L3, and L4) sequences (Fig. 2B, C, and D). Moreover, branch distances are very short, indicating a very low divergence rate between serum- and lymphocyte-derived glycoprotein genes (respectively, 99% and 96% sequence identity on average). On the other hand, the tree obtained for patient 1 sequences displays a clear and complete dichotomy between serum-derived sequences (named S1) and lymphocyte-derived sequences (named L1) branching separately (Fig. 2A). This strong compartmentalization indicates that all lymphocyte-derived viruses of patient 1 (L1) are monophyletic. Importantly, lymphocyte-derived glycoproteins are very divergent from serum-derived ones, with 67% sequence identity on average, and likely correspond to a different genotype. As patient 4 exhibited a low number of isolated sequences, a low E1E2 compartmentalization, and was infected by a viral genotype similar to that of patient 2, the following functional studies mainly focused on samples related to patient 1 (gt1b), 2 (gt2a), and 3(gt3a) (66 sequences, comprising 34 serum-derived sequences and 32 B-cell-derived sequences).

E1E2 sequences isolated from both serum and B lymphocytes allow the generation of HCVpp transducing hepatocyte cell lines. To assess E1E2 functionality and the potential tropism they provide, we generated HCV retroviral pseudoparticles (HCVpp) and analyzed the expression and incorporation of E1E2 envelope glycoproteins. We first analyzed by Western blotting the expression of the E1E2 envelope glycoproteins following cotransfection of HEK293T cells with a murine leukemia virus (MLV) Gag-Pol packaging construct and an MLV-based transfer vector encoding the green fluorescent protein (GFP). Overall, the isolated E1E2 sequences from patients 1, 2, and 3 were correctly expressed, with only few exceptions (Table 1). In parallel, pseudoparticles harboring the different E1E2 envelopes were purified from cell culture supernatant, and incorporation of E1E2 onto particles was evaluated by Western blotting. E1E2 incorporation onto HCVpp, as detected using the 3/11 or H52 anti-E2 antibodies, appeared more heterogeneous than expression among patients and compartments. Indeed, 33 out of 66 envelopes (Table 1) presented either a defect

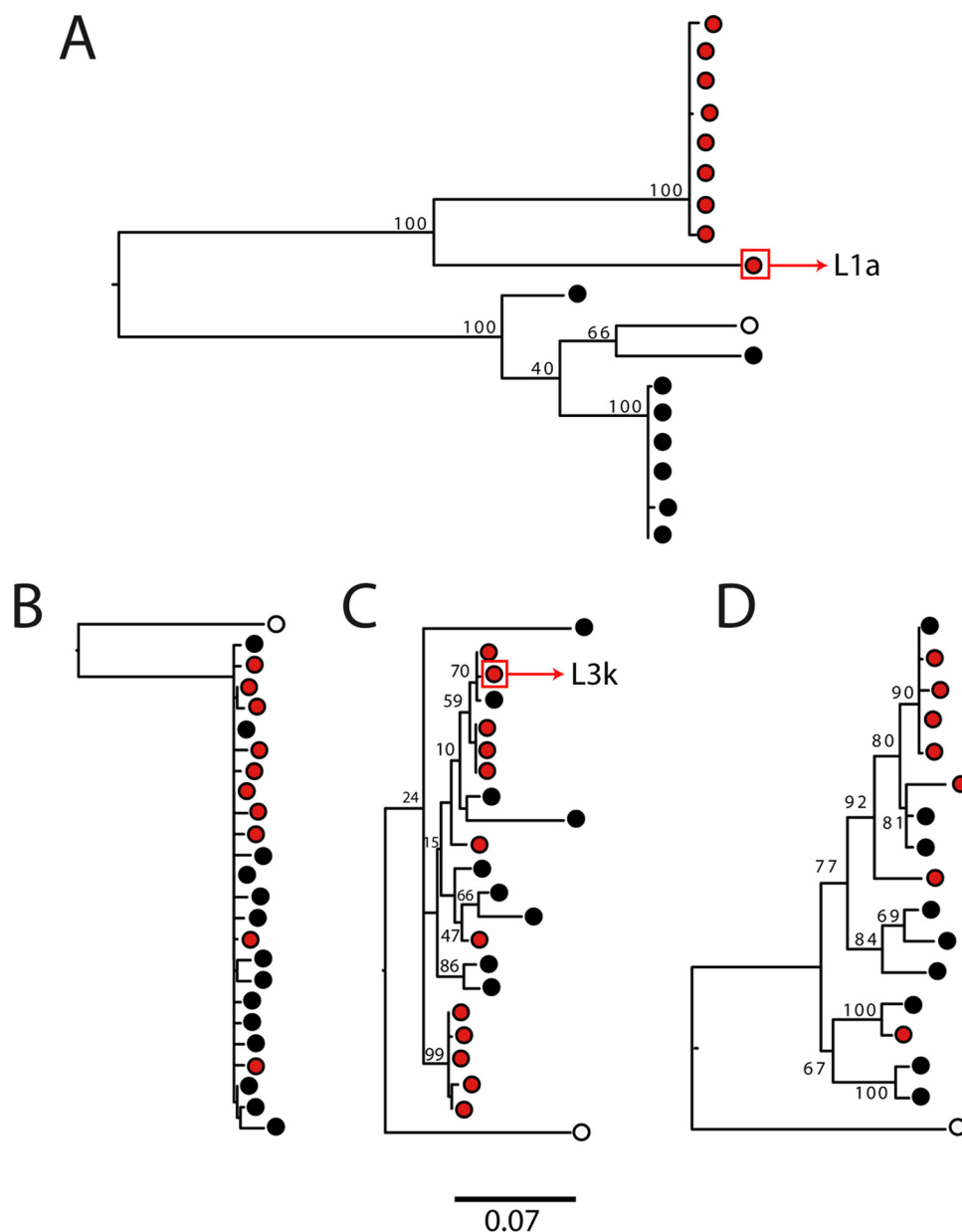


FIG 2 Phylogenetic analysis of E1E2 envelope glycoproteins. Maximum likelihood trees were computed for the E1E2 envelope glycoprotein amino acid sequences isolated from patient 1 (gt1b [A]), patient 2 (gt2a [B]), patient 3 (gt3a [C]), and patient 4 (gt2b [D]). The trees were rooted with the midpoint root, and the numbers indicate bootstrap values for the major nodes. Black dots represent serum-derived sequences, and red dots indicate B-lymphocyte-extracted sequences. White dots correspond to reference sequences of genotypes 1b, 2a, and 3a, respectively. The E1E2 envelopes this work particularly focuses on are boxed in red squares.

for incorporation or adopted a particular conformation onto HCVpp undetectable by our antibodies.

We then tested the functionality and potential of E1E2 to confer entry to HCVpp on Huh7.5 hepatoma cell lines (Fig. 3). Overall, HCVpp harboring patient 1 serum (S1) and B-lymphocyte-derived E1E2 sequences (L1) were able to transduce hepatoma cell lines more efficiently and significantly in comparison to patient 2- and 3-derived E1E2 sequences (S2, S3, and L3, $P < 0.05$; L2, $P = 0.053$) (Fig. 3A). (Raw infectious titers related to individual envelope glycoproteins are depicted in Fig. 3B.) Thus, the absence of incorporation onto viral particles of the L1 envelopes was likely

due to a particular conformation adopted by E1E2 sequences that is not recognized by the 3/11 or H52 anti-E2 antibodies (Table 1). Altogether, our data showed that 95% of patient 1 E1E2 sequences were fully functional to provide HCVpp entry into hepatocytes, whereas, respectively, 33% and 44% of the patient 2 and 3 E1E2 sequences allowed efficient HCVpp hepatocyte transduction (Fig. 3).

Chimeric HCVcc harboring lymphocyte-isolated E1E2 sequences (LyE1E2-HCVcc) are suboptimal for entry into hepatocyte cell lines. We then used HCVpp harboring the isolated E1E2 to infect different lymphocyte-derived cell lines, including two

TABLE 1 E2 expression in transfected 293T cells and E2 incorporation on concentrated pseudoparticles of the different envelope glycoproteins analyzed by Western blotting using the 3/11 or H52 antibodies to detect E2 and p30 to detect MLV-CA

Envelope identification no.	Result for ^a :	
	Expression	Incorporation
Patient 1 (genotype 1b)		
S1a	++	++
S1b	++	++
S1c	++	++
S1d	+	ND
S1e	++	++
S1f	++	++
S1g	++	ND
S1h	++	++
L1a	++	ND
L1b	++	ND
L1c	++	ND
L1d	++	ND
L1e	++	ND
L1f	++	ND
L1g	++	ND
L1h	++	ND
L1i	++	ND
Patient 2 (genotype 2a)		
S2a	++	+
S2b	++	ND
S2c	++	+
S2d	++	++
S2e	++	++
S2f	++	++
S2g	++	++
S2h	++	ND
S2i	++	++
S2j	++	ND
S2k	++	ND
S2l	++	++
S2m	++	ND
S2n	++	ND
L2a	++	+
L2b	++	+
L2c	++	+
L2d	ND	ND
L2e	+	ND
L2f	+	++
L2g	++	ND
L2h	++	+
L2i	++	+
L2j	+	ND
Patient 3 (genotype 3a)		
S3a	++	+
S3b	++	ND
S3c	++	+
S3d	++	++
S3e	ND	ND
S3f	++	+
S3g	+	ND
S3h	++	++
S3i	++	++
S3j	++	+
S3k	++	ND
S3l	++	+
L3a	+	ND

TABLE 1 (Continued)

Envelope identification no.	Result for ^a :	
	Expression	Incorporation
L3b	ND	ND
L3c	++	+
L3d	++	+
L3e	ND	ND
L3f	+	ND
L3g	++	ND
L3h	++	ND
L3i	++	ND
L3j	++	+
L3k	++	++
L3l	+	+
L3m	+	+

^a ++ similar to the level of wild-type E1E2 from the same genotype; + weak expression or incorporation; ND nondetectable.

B-lymphocyte cell lines (Raji and Daudi), one T-lymphocyte cell line (Molt4), and one chimeric B/T-lymphocyte cell line (X174). Viral entry was not detectable or was poorly detectable for all of the E1E2 envelopes and cell lines tested (Fig. 4). When detectable, entry was restricted to HCVpp harboring particular L1 envelopes (such as for HCVpp L1a or L1g), but such a phenomenon was partially reproducible over the experiments, thus highlighting the need to pursue the characterization of such envelopes with a more suitable infection system. Even though HCVpp represents a good model for testing the functionality of E1E2 complexes, these particles do not recapitulate properly the cell entry and assembly pathways of HCV particles. A major concern is that HCVpp do not interact with the lipoprotein metabolism, a critical regulator of the HCV entry and replication cycle. To overcome these limitations, we then used a cell-culture-derived HCV (HCVcc JFH-1/H77 molecular clone), which recapitulates the proper HCV entry pathway, as a platform for properly assessing the impact of B-lymphocyte-isolated E1E2 sequences on HCV entry tropism. For this purpose, we constructed chimeric cell-culture-derived HCV virus expressing either a strongly compartmentalized B-lymphocyte-isolated E1E2 sequence from patient 1 (L1a E1E2; HCVcc designated L1a/JFH1) or a poorly compartmentalized E1E2 sequence from patient 3 (L3k E1E2; HCVcc designated L3k/JFH1) (Fig. 2A and D).

Following electroporation of the Huh7.5 hepatoma cell line with LyE1E2-HCVcc, HCVcc H77/JFH-1, and ΔE1E2/JFH-1 RNAs, cell culture supernatant was harvested at 48 and 72 h post-electroporation in order to assess viral particle production and supernatant infectious titers. Cell culture supernatants from Huh7.5 cells electroporated with LyE1E2-HCVcc RNA were poorly infectious on Huh7.5 cells at 48 h and 72 h postelectroporation, in contrast to cell supernatant containing the prototype H77/JFH1 HCVcc (Fig. 5A). Consistently, quantification of genome-equivalent viral particles (i.e., RNA copy number per milliliter) over time following electroporation showed that LyE1E2-HCVcc viruses did not propagate as efficiently as HCVcc H77/JFH-1 in cell culture (Fig. 5B). However, the impaired infectivity of LyE1E2-HCVcc could not be resumed due to differences in viral particle production at a specific time point (Fig. 5B) or differences in viral particle release (Fig. 5C). Indeed, determination of the L1a/JFH1 and L3k/JFH1 virus-specific infectivity underlined that their impaired hepatotropism was mainly due to an entry defect (Fig. 5D).

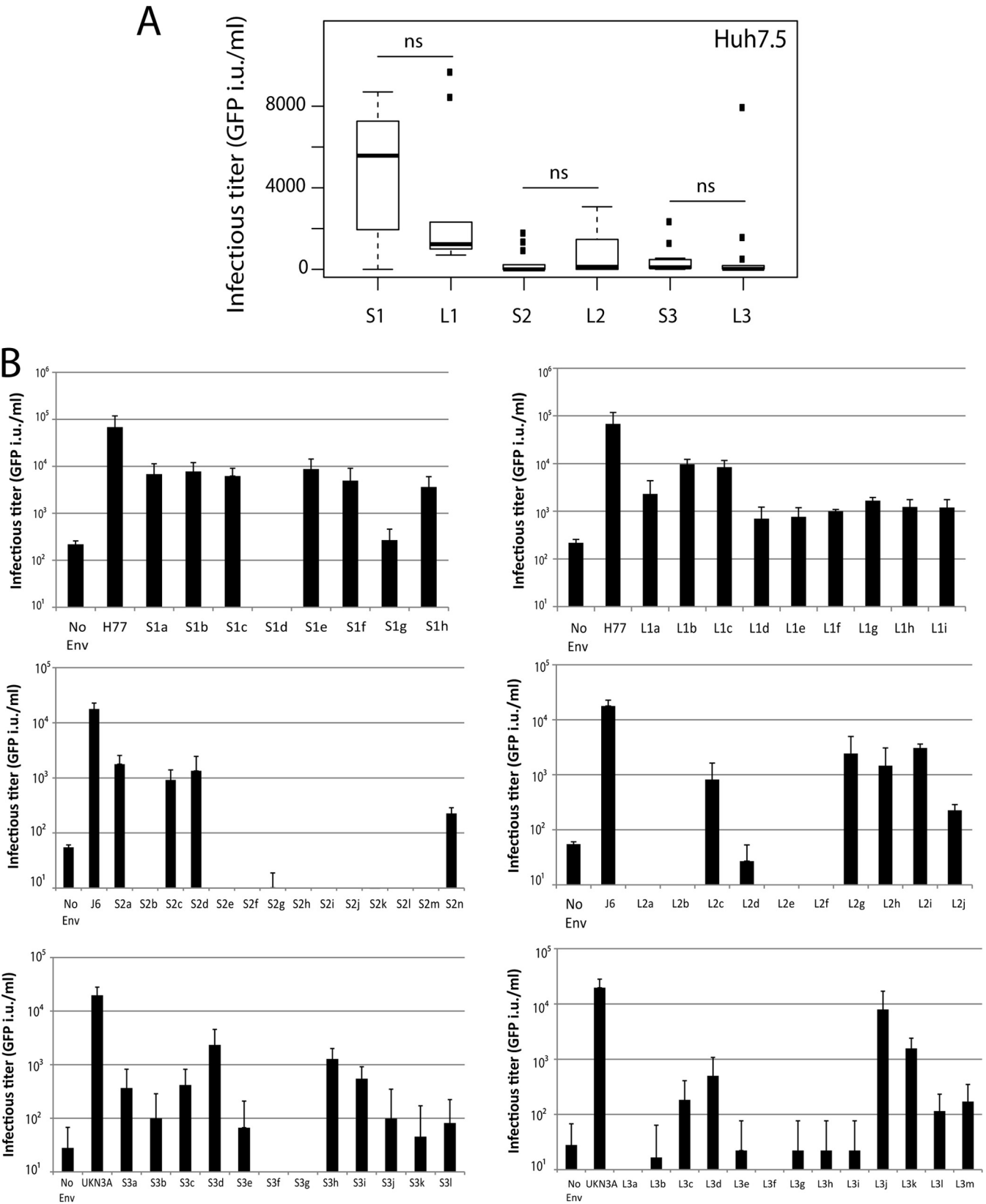


FIG 3 Hepatotropism of HCVpp harboring the isolated E1E2. (A) Box and whisker representation of infectious titers on Huh-7.5 of HCVpp harboring E1E2 isolated from a same compartment and patient. HCVpp harboring E1E2 isolated from serum (S1 to S3) or B lymphocytes (L1 to L3) of patient 1, patient 2, or patient 3 were used to infect Huh7.5 and distribution of HCVpp infectious titers for each patient compartment were calculated. HCVpp infectious titers were not normalized with “no env” infectivity values, as normalization had no impact on presented distribution profiles. Results are expressed as infectious units (i.u.) per

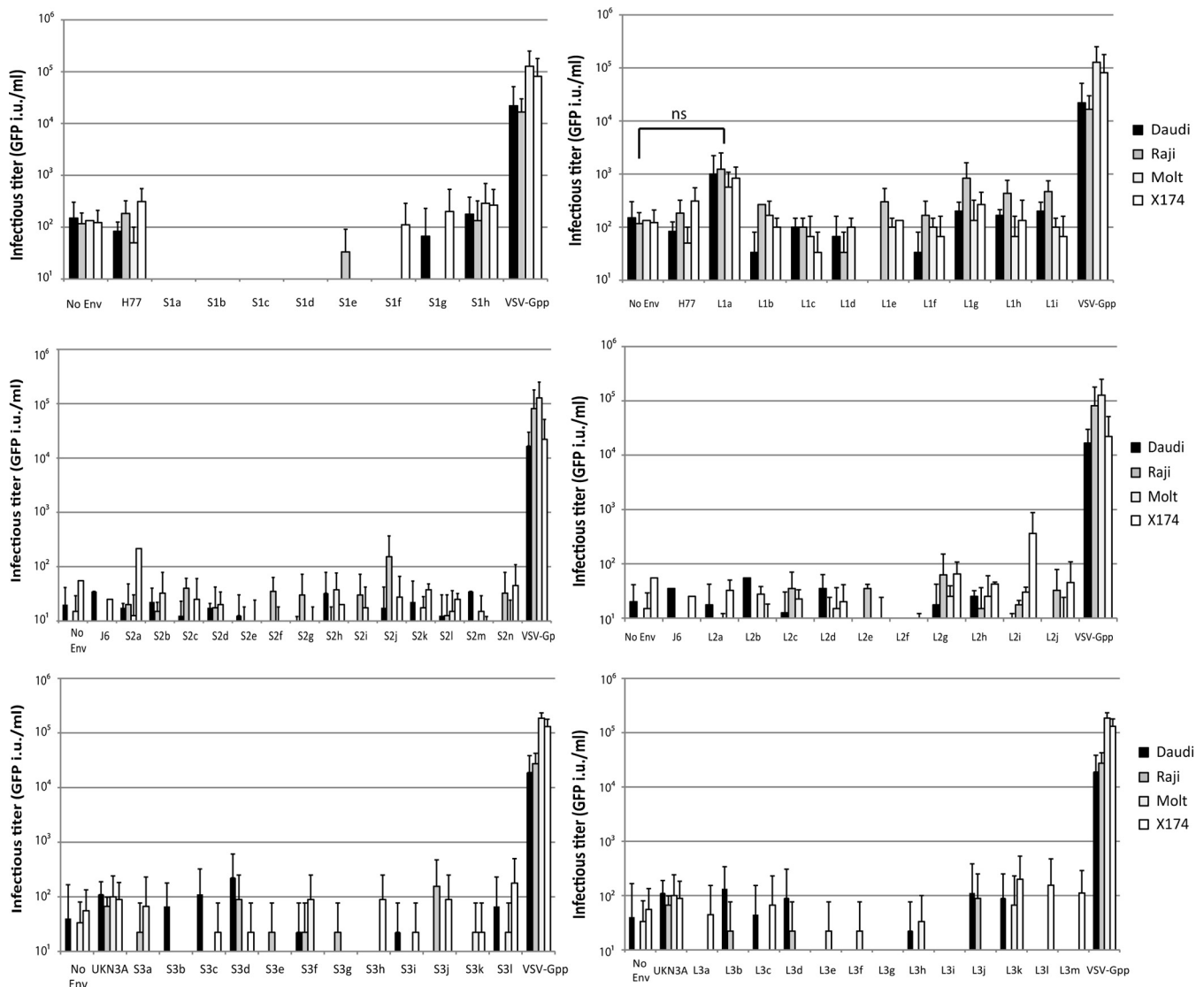


FIG 4 Related lymphotropism of serum- and B-lymphocyte-derived envelope glycoproteins. HCV entry assays using HCVpp harboring serum (S)- or B-lymphocyte (L)-derived envelope glycoproteins from patient 1 (S1x or L1x), patient 2 (S2x or L2x), and patient 3 (S3x or L3x). Each envelope glycoprotein in a patient and compartment is identified by a lowercase letter. Raji, Daudi, Molt, and X174 cells were inoculated with HCVpp harboring the indicated envelope glycoproteins or no glycoprotein (no Env), and infectivity titers were determined by flow cytometry 72 h after inoculation. HCV pseudoparticles harboring E1E2 from gt1a H77 (noted 7a, [AF009606](#)), gt2a J6 (noted J6; [AF177036.1](#)) or gt3a UKN3a1.28 (noted UKN3; [AY734984](#)) were used as controls. Results represent average infectious titers, expressed as infectious units (i.u.) per milliliter (mean \pm SD; $n = 4$; ns, not significant).

HCVcc harboring compartmentalized LyE1E2 sequences preferentially enter into B lymphocytes. In order to determine whether the impaired entry tropism of L1a/JFH1 and L3k/JFH1 HCVcc into hepatocyte cell lines can be explained by lymphotropic specialization of these E1E2 sequences, we infected Raji cell

lines (non-Hodgkin's B-lymphoma cell lines) with JFH-1 HCVcc viruses expressing different envelope glycoproteins (H77, L1a, and L3k) or not (Δ E1E2). Raji cells were infected with equivalent amounts of HCV particles following quantification of genome equivalent physical particles by RT-qPCR. Strikingly, the level of

milliliter. For each patient compartment, the bottom and top of the boxes represent the 25th and 75th percentiles, respectively, and the bold lines within boxes represent the HCVpp infectivity median. The top (maximum value) and bottom (minimum value) of the whiskers represent the HCVpp infectivity standard deviation (SD) for each patient compartment. Black dots located above the top of the whiskers represent the outlier or far-outlier values of the distributions. (B) HCV entry assays using HCVpp harboring serum (S)- or B-lymphocyte (L)-derived envelope glycoproteins from patient 1 (S1x and L1x), patient 2 (S2x and L2x), and patient 3 (S3x and L3x). Each envelope glycoprotein in a patient and compartment is identified with a minuscule letter. Huh-7.5 cells were inoculated with HCVpp harboring the indicated envelope glycoproteins or no glycoprotein (no Env), and infectivity titers were determined by flow cytometry 72 h after inoculation. HCV pseudoparticles harboring E1E2 from gt1a H77 (designated 7a [[AF009606](#)]), gt2a J6 (designated J6 [[AF177036.1](#)]), or gt3a UKN3a1.28 (designated UKN3 [[AY734984](#)]) are used as positive controls of infection. Results represent average infectious titers, expressed as infectious units (IU) per milliliter (mean \pm SD; $n = 4$).

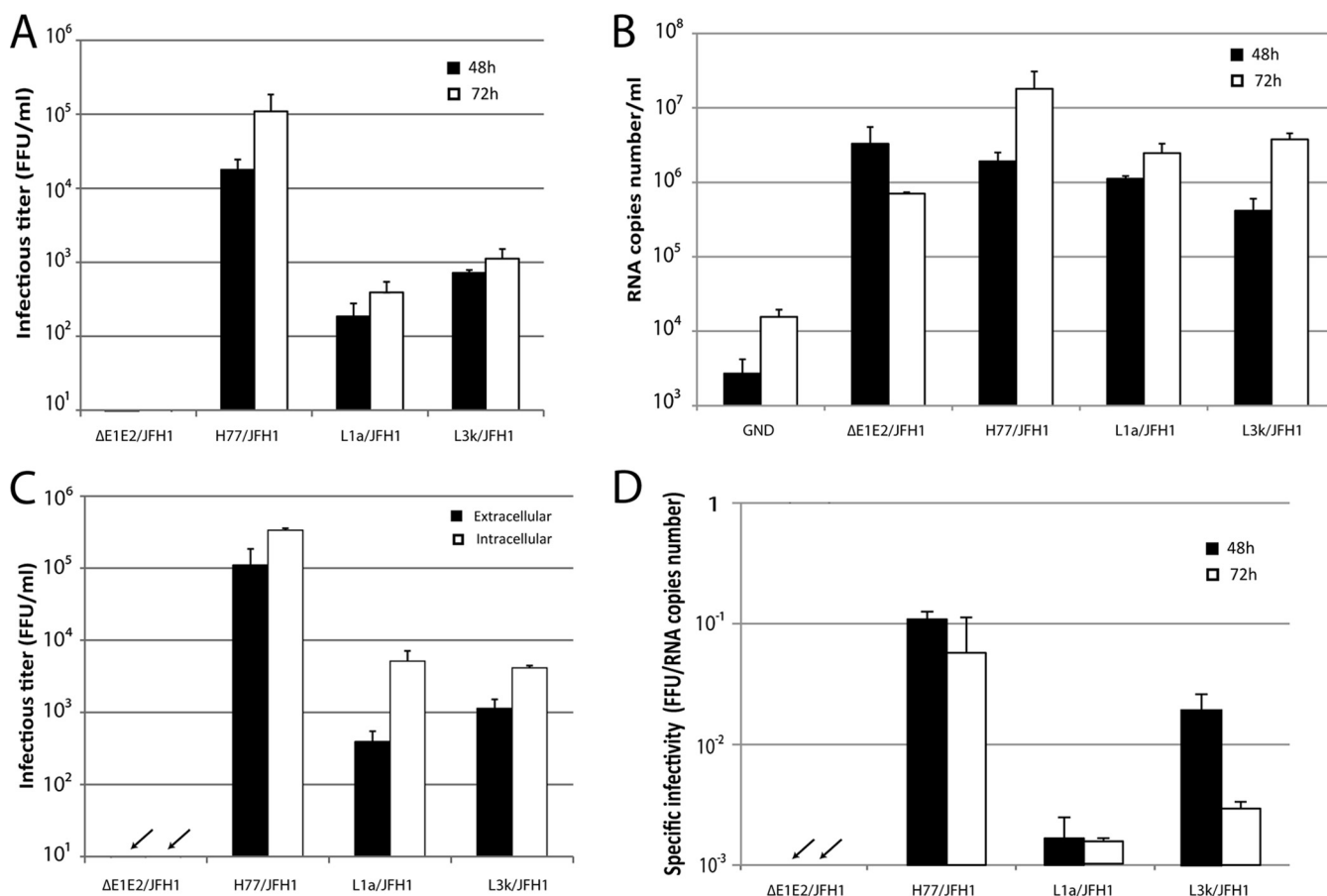


FIG 5 Production and characterization of the LyE1E2-HCVcc viruses. HCVcc particles harboring the H77, L1a, or L3k envelope glycoproteins or encoding a genome deleted for E1 and E2 (Δ E1E2) were harvested at 48 h and 72 h after electroporation of Huh7.5 cells and analyzed for HCV infectivity by titration on naive Huh-7.5 cells. Titters are expressed as focus-forming units (FFU) per milliliter (mean \pm SD; $n = 4$) (A) and RNA copies as HCV RNA genome equivalent (GE) levels determined by qRT-PCR (B). A replication (GND)-defective genome was used as a negative control for quantification of viral RNA. (C) Intracellular and extracellular infectious titers of HCVcc viral particles harboring the different E1E2 at 72 h after electroporation. Viral particles were harvested either from cell supernatant (extracellular infectivity) or after disruption of producer cell membranes (intracellular infectivity) and titrated on naive Huh-7.5 cells. Results are expressed as focus-forming units per milliliter (mean \pm SD; $n = 3$). (D) Specific infectivity of HCVcc viral particles harboring the three different envelope glycoproteins was calculated as infectivity per HCV RNA GE at 48 h and 72 h postelectroporation.

cell-associated viral RNA (normalized on the GAPDH mRNA level) was significantly higher when Raji cells were incubated with LyE1E2-HCVcc viruses, in contrast to Raji cells incubated with Δ E1E2/JFH1 or with H77/JFH1 HCVcc (Fig. 6A). Such preferential association was also confirmed through independent isolation and reverse transcription of cell-associated viral RNA from infected Raji cells. Indeed, by using two successive nested PCRs, we successfully managed to amplify E1E2 cDNA fragments from only L1a/JFH1- and L3k/JFH1-infected Raji cells (Fig. 6B). No viral E1E2 sequence could be amplified for the other conditions, highlighting a clear correlation between viral RNA amplification and the origin of E1E2 envelope. Consistently with the fact that JFH-1 cannot productively replicate (B cells do not express the HCV replication-dependent, liver-specific microRNA miR-122) and produce viral particles within PBMCs (25), no significant production of *de novo* physical particles could be detected in Raji cell supernatants for any virus (Fig. 6C).

We then sought to determine whether the presence (or absence thereof) of viral RNA in B cells was associated with viral protein expression. A reproducible expression of the viral an-

tigen NS5A could be detected in Raji cells infected with LyE1E2-HCVcc viruses in contrast to cells infected with Δ E1E2/JFH1 or with H77/JFH1 HCVcc (Fig. 6D). The percentage of Raji cells positive for NS5A were significantly higher following incubation with LyE1E2-HCVcc viruses (L1a, 6.47%; L3k, 4.67%; $P < 0.001$) than after incubation with H77/JFH1 HCVcc (3.11%) (Fig. 6D). Altogether, NS5A expression within Raji cells ruled out the possibility that E1E2 lymphotropism was resumed in our experimental settings due to an association between viral particles and B-lymphocyte cell surface molecules. In contrast, this result underlined that LyE1E2-HCVcc viruses were able to induce the expression of a viral protein into B lymphocytes in an E1E2-dependent manner despite the absence of viral particle production. We then determined the ratio between Huh7.5-specific infectivity and Raji infectivity (i.e., Raji infectious titers based on the percentage of NS5A-positive Raji cells) of each envelope in order to quantify their respective lymphotropism. Interestingly, the L1a envelope appeared significantly more lymphotropic than the L3k envelope (Fig. 6E), thus strongly highlighting a correlation between the

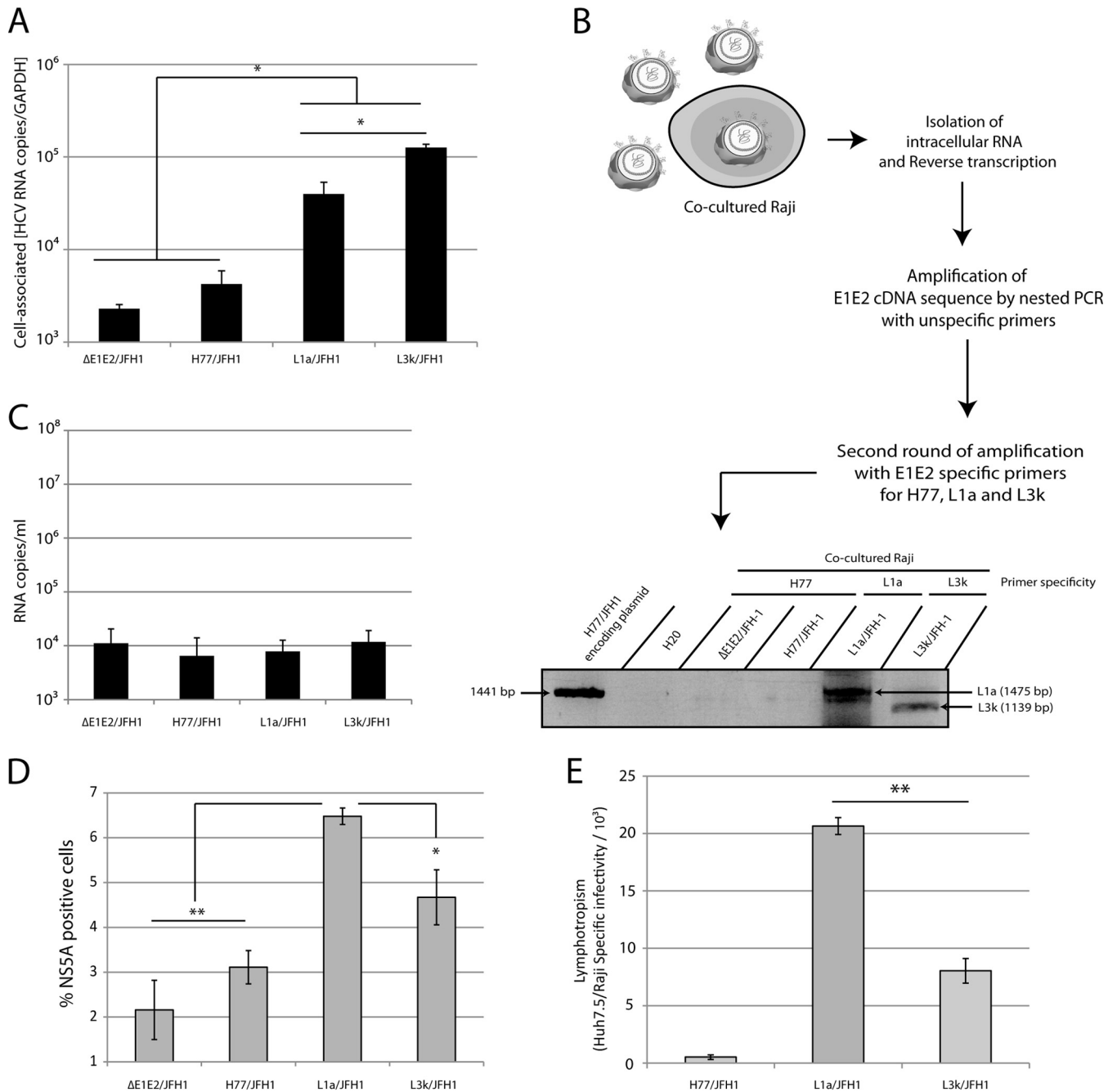


FIG 6 Characterization of the LyE1E2-HCVcc lymphotropism. (A) Quantification of cell-associated viral RNA following Raji cell infection with HCVcc harboring the different E1E2 proteins (H77, L1a, and L3k) or no E1E2 (Δ E1E2). Four days postinfection, Raji cells were harvested and lysed, and total RNA was extracted. The amounts of cell-associated viral RNA for each infection were then determined by RT-qPCR and normalized with the GAPDH mRNA expression level (mean \pm standard deviation [SD]; $n = 4$). *, $P < 0.05$. (B) Amplification of E1E2 sequences isolated from infected Raji cells. Following infection, intracellular RNAs were isolated from Raji cells and reverse transcribed. E1E2 sequences were then amplified by nested PCR with E1E2 outer unspecific and inner specific primers (for each construct H77, L1a, L3k, and Δ E1E2). The HCVcc-encoding plasmid pFK H77/JFH1/HQL was used as a control of amplification. (C) Quantification of viral RNA within Raji cell culture supernatants following infection with HCVcc harboring the different E1E2 proteins (H77, L1a, and L3k) or no E1E2 (Δ E1E2). Cell supernatants were harvested 4 days postinfection, and the level of viral RNA was quantified by RT-qPCR (mean \pm SD; $n = 4$). (D) Expression of NS5A viral protein within Raji cells infected by the different HCVcc viruses. The percentage of NS5A-positive Raji cells following infection with HCVcc harboring the different E1E2 proteins (H77, L1a, and L3k) or no E1E2 (Δ E1E2) were determined 4 days postinfection by measuring NS5A expression levels using flow cytometry (FACSCanto II; BD Biosciences) (mean \pm SD; $n = 4$). **, $P < 0.001$; *, $P < 0.05$. (E) Lymphotropism of the different HCVcc virus. The average ratios between Huh-7.5-specific infectivity (Fig. 5D) and Raji infectivity (Raji infectious titers calculated based on the percentage of NS5A-positive cells) (Fig. 6D) for each HCVcc virus were calculated (mean \pm SD; $n = 4$). **, $P < 0.001$.

degree of lymphotropism and the degree of phylogenetic segregation.

LyE1E2-HCVcc virus entry into B cells occurs via an endocytosis, pH-dependent process. HCV entry into hepatocytes is regulated by several viral and cellular mediators. To challenge the ability of the LyE1E2-HCVcc viruses to enter into B cells, as well as to characterize some features of this phenomenon, we aimed to inhibit LyE1E2-HCVcc virus entry into Raji cells. Following viral particle internalization, the release of the viral RNA into the cell cytosol follows the merging of virus and endosome membrane ("membrane fusion"). Such fusion is dependent of several E1E2 conformational changes that are triggered by E1E2 receptor interactions and endosomal acidification. Bafilomycin A1 has been shown to inhibit HCV fusion through blocking of the acidification of early endosome (35). Thus, we sought to test the impact of the bafilomycin A1 on LyE1E2-HCVcc virus entry into B cells in order to demonstrate the role of E1E2 in this process. We first assessed the ability of bafilomycin A1 to inhibit entry of pseudoparticles harboring VSV-G envelope glycoproteins (VSVGpp) into Raji cells. Incubation of Raji cells with 10 nM and 25 nM bafilomycin before (30 min) and during (6 h) infection totally abrogated entry of VSVGpp, as detected by the absence of GFP expression into Raji cells 4 days postinfection (Fig. 7A). In parallel, a concentration of 50 nM appeared to be toxic for the cells. Following pretreatment with 20 nM bafilomycin, Raji cells were then infected with equivalent amount of HCVcc virus (Δ E1E2/JFH1, H77/JFH1, L1a/JFH1, or L3k/JFH1) premixed with 20 nM bafilomycin A1. Four days postinfection, cells were lysed, and cell-associated viral RNA was quantified by one-step RT-qPCR. Viral RNA levels were normalized on GAPDH mRNA expression level to account for any cell toxicity effect due to bafilomycin A1 treatment. Moreover, we also ascertained the absence of strong cytotoxic effect of bafilomycin A1 on cell viability and cell surface molecule expression during the course of infection by quantifying Raji cell viability and CD81 cell surface expression (Fig. 7B). Importantly, the amount of LyE1E2-HCVcc viral RNA was significantly reduced in Raji cells treated with bafilomycin A1 in contrast to DMSO-treated cells (Fig. 7C). In parallel, levels of H77/JFH1 RNA within B cells remained unchanged by bafilomycin A1 treatment. Overall, these results highlighted that LyE1E2-HCVcc virus enters specifically into B cells through an E1E2-mediated, pH-dependent process as hepatotropic HCV variants.

Several cell surface molecules have been previously demonstrated to be critical for HCV entry into hepatocytes. Thus, we next sought to analyze the impact of CD81 on HCV entry into B cells, a critical HCV receptor in the liver that is significantly expressed by Raji cells (Fig. 7B). Following preincubation with an anti-CD81 antibody known to inhibit HCV binding (36), Raji cells were infected with equivalent amount of HCVcc virus (H77/JFH1, L1a/JFH1, or L3k/JFH1) or with HCVcc encoding no envelope glycoprotein (Δ E1E2/JFH1). Four days postinfection, no significant reduction of viral RNA could be observed in Raji cells infected by LyE1E2-HCVcc and treated with JS81 anti-CD81 antibody in comparison to infected, nontreated cells (Fig. 7D). The ability of the anti-CD81 antibody JS81 to efficiently bind CD81 at the Raji cell surface in the same experimental settings was controlled in parallel (Fig. 7E).

Overall, the absence of entry neutralization by the anti-CD81 antibody suggests that LyE1E2-HCVcc viruses use alternative entry routes and receptors prior to internalization into B cells. Sur-

prisingly, entry of L1a/JFH-1 HCVcc was slightly but significantly enhanced when CD81 was blocked (Fig. 7D), suggesting that particular lymphotropic strains may have conserved a residual affinity for CD81. The potential ability of CD81 to hamper the entry of particular LyE1E2-HCVcc viruses into B cells supports the idea that such entry is both a specific and CD81-independent process.

A global phylogenetic analysis highlights the existence of variants from two different genotypes segregating between serum and B cells in patient 1. To investigate the global genetic diversity of isolated E1E2 proteins, we conducted a global phylogenetic analysis of all isolated sequences. We also added reference sequences of additional genotypes and of the envelope glycoprotein of the SB strain. The HCV SB strain has been isolated from a B-cell line derived from a patient with non-Hodgkin's lymphoma, and HCV SB strain virus has been found to slightly infect PBMCs (22). Interestingly, L1 and S1 E1E2 amino acid sequences were not found to be monophyletic (Fig. 8A), in contrast to E1E2 sequences from patients 2 and 3, supporting their origins from different genotypes. A tree computed on the nucleotide alignment gave similar results (Fig. 8B). The S1 sequences clearly appear to belong to genotype 1b, whereas the L1 sequences are more related to genotype 2 sequences (Fig. 8). Interestingly, L1a's closest relative is the B-cell-line-derived E1E2 sequence from the SB strain (88% identical), which is also related to genotype 2b (22), thus suggesting a potential ability of genotype 2 viruses to become more easily lymphotropic than other genotypes. The clear segregation in each compartment of the two distinct genotypes indicates a strong specialization of each genotype in patient 1. This strict phylogenetic compartmentalization, much stronger than those previously reported for shorter segments (12, 13, 18, 23), highly supports the fact that the lymphocyte-derived viruses from patient 1 could harbor significant specialization for lymphocyte infection *in vivo*.

We then took advantage of the close proximity of the L1 sequences with the sequence of reference of gt2b (Ref2b; characterized as hepatotropic) to assess the presence of potential specific mutations within L1 sequences. Interestingly, amino acid sequence alignments of three L1 sequences (L1a, L1b, and L1i; the L1b to L1i sequences are highly similar) with the Ref2b sequence highlighted six major amino acid substitutions within the L1 group in comparison to Ref2b sequence (Fig. 9). These substitutions were either similar (R106Y, T137P, H204R, K218Q, and E333R) or equivalent in term of polarity or hydrophobicity modifications (G271N/E). Interestingly, these substitutions were found at the same positions within the SB sequence. Among them, three substitutions were similar to L1 sequences (T137P, H204R, and K218Q), and two substitutions were equivalent in terms of polarity (G271R and E333K). Thus, these residues could represent a visible piece of the combination of substitutions that could characterize the lymphotropism of genotype 2b-E1E2 sequences.

DISCUSSION

HCV lymphotropism has remained for a long time a controversial and poorly understood phenomenon. Even though it is certain that HCV infection of PBMCs does not represent a major site of viral replication *in vivo* in comparison to the liver, considerable evidence over recent years has shown that such side events can be now significantly detected in patients and in some cases have an effect on pathogenesis. However, the molecular characterization of this phenomenon still remains to be achieved. In this study, we analyzed for the first time the genetic compartmentalization of full

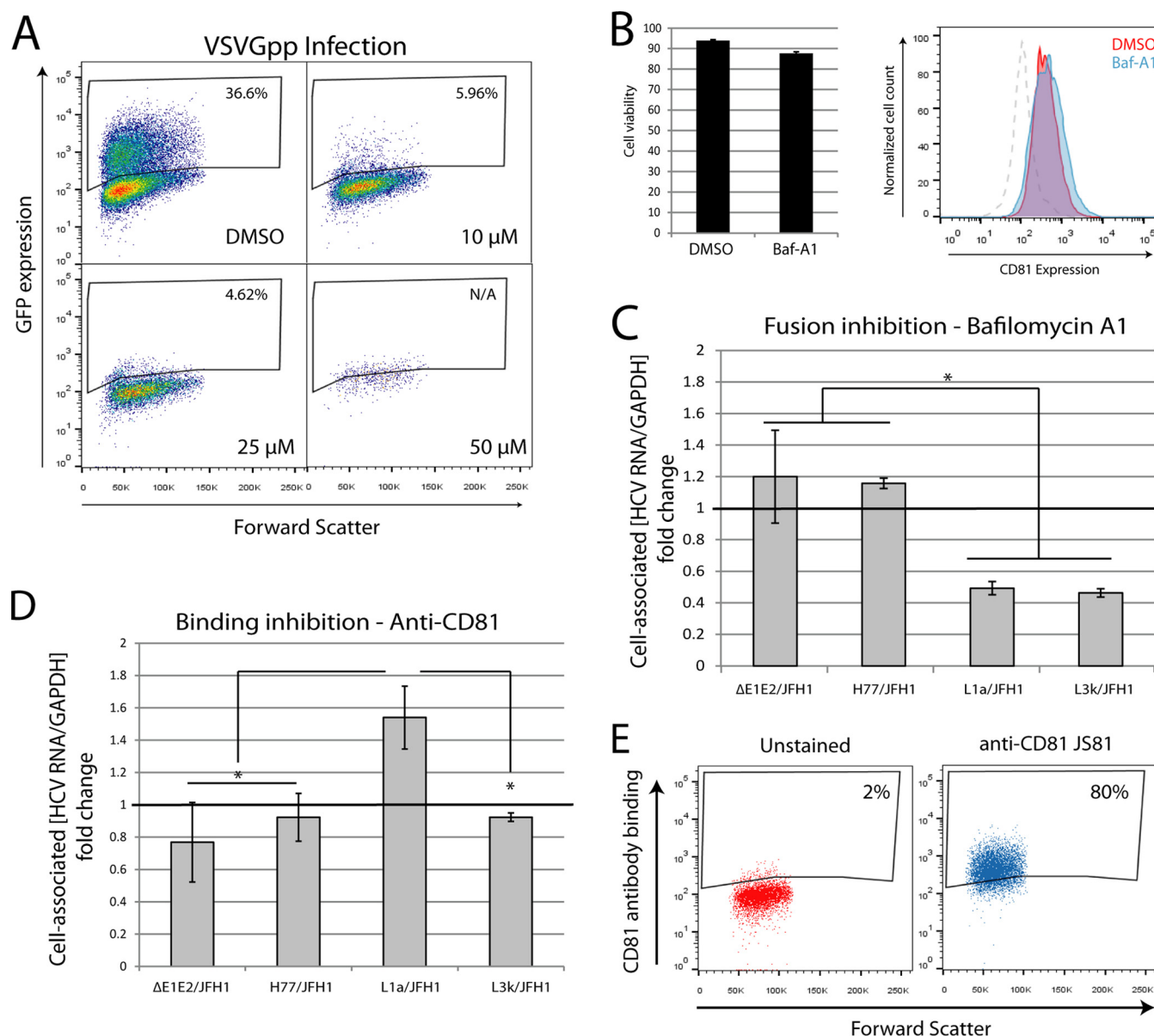


FIG 7 Effect of bafilomycin A1 and anti-CD81 JS81 antibody on LyE1E2-HCVcc entry into Raji cells. (A) Impact of bafilomycin A1 on VSVGpp entry into Raji cells. Following pretreatment with DMSO or with respective concentrations of bafilomycin A1 (10, 25, or 50 μ M), Raji cells were infected at 37°C with an equivalent amount of VSVGpp premixed with the respective concentration of bafilomycin A1 (DMSO). Six hours later, cells were washed, and GFP expression was assessed 4 days later by flow cytometry. (B) Raji cell viability (left) and cell surface expression of CD81 at Raji cell surface (right) following bafilomycin treatment. Following a 4-day treatment with DMSO or 20 μ M bafilomycin A1, Raji cells were stained with propidium iodide or anti-CD81 antibody. Cell death and CD81 expression levels were quantified by flow cytometry. (C) Raji cells were infected with HCVcc harboring the different E1E2 proteins (H77, L1a, and L3k) or no E1E2 (Δ E1E2) in the presence of DMSO or 20 μ M bafilomycin A1. Four days postinfection, Raji cells were harvested, lysed, and total RNA were extracted. Amounts of cell-associated viral RNA for each infection were then determined by RT-qPCR and normalized with the GAPDH mRNA expression level. Results are presented as cell-associated viral RNA fold change relatively to viral RNA levels detected in Raji cells treated with DMSO (mean \pm SD; $n = 4$), $P < 0.05$. (D) Efficiency of CD81 neutralization by the anti-CD81 antibody JS81 prior to HCVcc infection. Raji cells were incubated for 1 h with the anti-CD81 antibody JS81 or not prior to infection with HCVcc harboring the different E1E2 proteins (H77, L1a, and L3k) or no E1E2 (Δ E1E2). Four days postinfection, cell-associated viral RNA fold changes were determined as described above (mean \pm SD; $n = 4$), $P < 0.05$. (E) CD81 cell surface expression in Raji cells after 1 h of anti-CD81 treatment and measured as in panel B.

HCV E1E2 sequences in four chronically infected patients. We observed that one patient (patient 1) presented a genetic compartmentalization between E1E2 sequences isolated from serum and B lymphocytes, suggesting their strong specialization. In contrast, the three other patients displayed no or very poor compartmentalization of HCV E1E2, likely reflecting different lymphotropism

features among genotypes or infection stages. Expression of L1a and L3k envelopes at the HCVcc JFH-1 virus surface was able to confer to this virus the ability to enter B cells, and viral entry appeared to be dependent on endosomal acidification. Finally, the level of lymphotropism of L1a/JFH-1 and L3k/JFH-1, determined through their ability to enter into Huh7.5 and Raji cells, high-

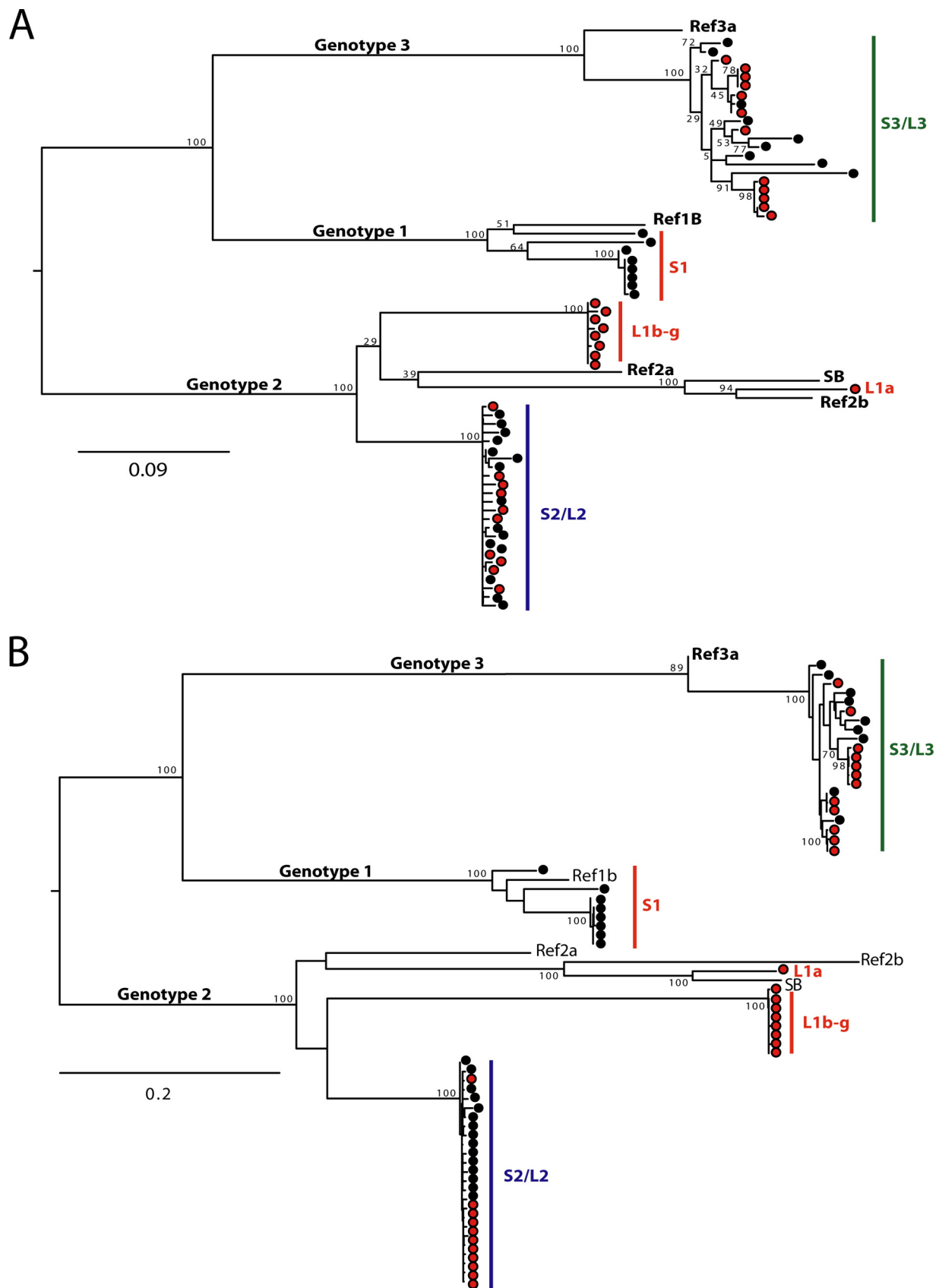


FIG 8 General phylogenetic analysis of E1E2 amino acid and nucleotide sequences. Phylogenetic trees depicting the general compartmentalization of E1E2 amino acids (A) and nucleotide (B) sequences are shown. The maximum likelihood tree was rooted with the midpoint root. Bootstrap values are indicated for the main nodes. Reference sequences 1b, 2a, 2b, and 3a were included in the analysis. Black dots indicate serum-derived sequences, and red dots correspond to B-lymphocyte-extracted sequences. White dots correspond to reference proteins of genotypes 1b, 2a, 2b, and 3a.

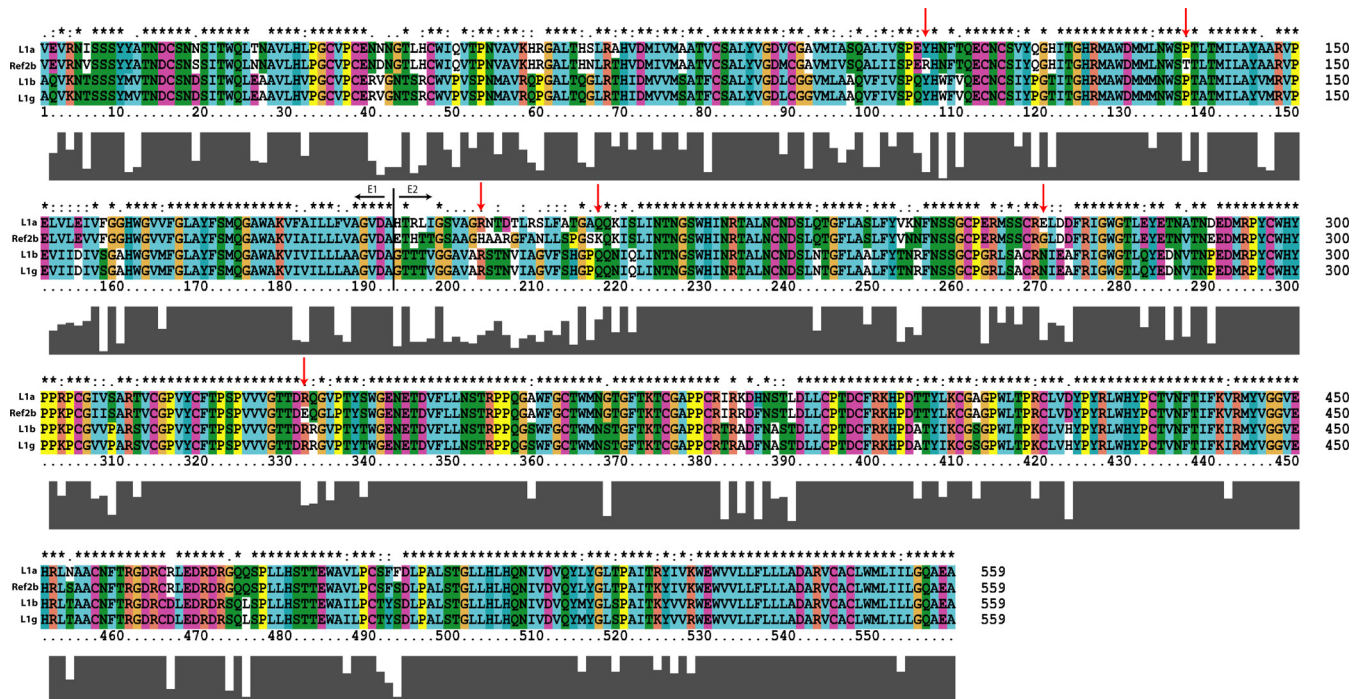


FIG 9 Amino acid alignment of L1 sequences with the Ref2b sequence. As L1b-to-L1i sequences harbor a high degree of similarities, only two sequences representative of this group were aligned (L1b and L1g) with L1a and Ref2b. Levels of conservation of amino acids are indicated. E1 and E2 sequences are separated by a bold vertical line. Colors indicate physicochemical similarities between amino acids. R106Y, T137P, H204R, K218Q, G271N/E, and E333R are indicated by red arrows.

lighted a correlation between the degree of envelope compartmentalization and lymphotropism. Altogether, our results support the existence in chronically infected patients of specialized HCV variants able to enter into B cells through a specific, E1E2-dependent process. Our findings are consistent with previous studies showing that slight entry of HCV patient-derived particles can be detected within PBMCs (3, 4, 12–16, 18, 21) in contrast to the JFH-1 virus (24).

The close genetic proximity of the L1a E1E2 proteins to the envelope glycoproteins from the lymphotropic SB virus (22), isolated from a different patient from another continent, reinforced the assumption that L1a E1E2 proteins carry important lymphotropism determinants. Here, we have highlighted a few amino acids that could represent potential mediators of HCV lymphotropism. However, the complete mapping of E1E2 lymphotropic determinants encounters several difficulties. First, it is likely that, with regard to the important genetic diversity between HCV genotypes, the E1E2 lymphotropism is mediated by a particular genetic combination of critical mutations in a genotype-dependent manner. Second, the complete identification of the genetic combination within genotypes would require the analysis and characterization of an important number of sequences. In the future, the characterization of the role in HCV lymphotropism of the amino acids pointed out by our study, combined with the isolation and analysis of more B-cell-derived genotype 2b HCV sequences (E1E2 but not limited to E1E2), could provide a better characterization of the HCV lymphotropic determinants.

Even though the L3k envelope was less lymphotropic than the L1a one (Fig. 6E), this envelope was able to confer to JFH-1 a significant ability to enter into B cells despite a poor genetic com-

partmentalization. Hence, the low degree of compartmentalization of L3k could also reflect the overall weak lymphotropism of the related quasiespecies despite potent entry ability. Indeed, these viruses may carry genetic determinants that are poorly adapted for productive infection of B-lymphocytes, hence making viral entry a dead end for these variants.

The low compartmentalization and divergence rate of lymphocyte-derived viruses of patients 2, 3, and 4 suggest that these viruses have been very recently and independently acquired from serum-derived viruses, during multiple contamination events. In contrast, the higher specialization for B-lymphocyte entry of the L1 E1E2 sequences supports the view that the entire genome of the corresponding quasiespecies is likely adapted for replication and viral particle production in B lymphocytes. Consistently, HVR1 and IRES sequences have already been shown to display a strong and marked genetic compartmentalization *in vivo* between B lymphocytes and serum-derived sequences (12, 23). In this study, the LyE1E2-HCVcc virus infectious cycle within B cells was restricted to virus entry and protein translation. Thus, the identification of additional genetic adaptations within nonstructural proteins of lymphocyte-derived variants could provide valuable information to assess if, and to what extent, HCV lymphotropic variants can replicate and produce *de novo* viral particles in B cells. Previous reports demonstrating that efficient HCV replication is dependent on the liver-specific microRNA mir122 (37) likely argue in favor of low HCV replication within B cells. Thus, the existence of adaptive mutations favoring HCV lymphotropic variants to escape the miR-122 requirement for replication remains to be demonstrated.

The ability of bafilomycin A1 to inhibit LyE1E2-HCVcc virus entry into B cells strongly suggested that entry into B cells is a

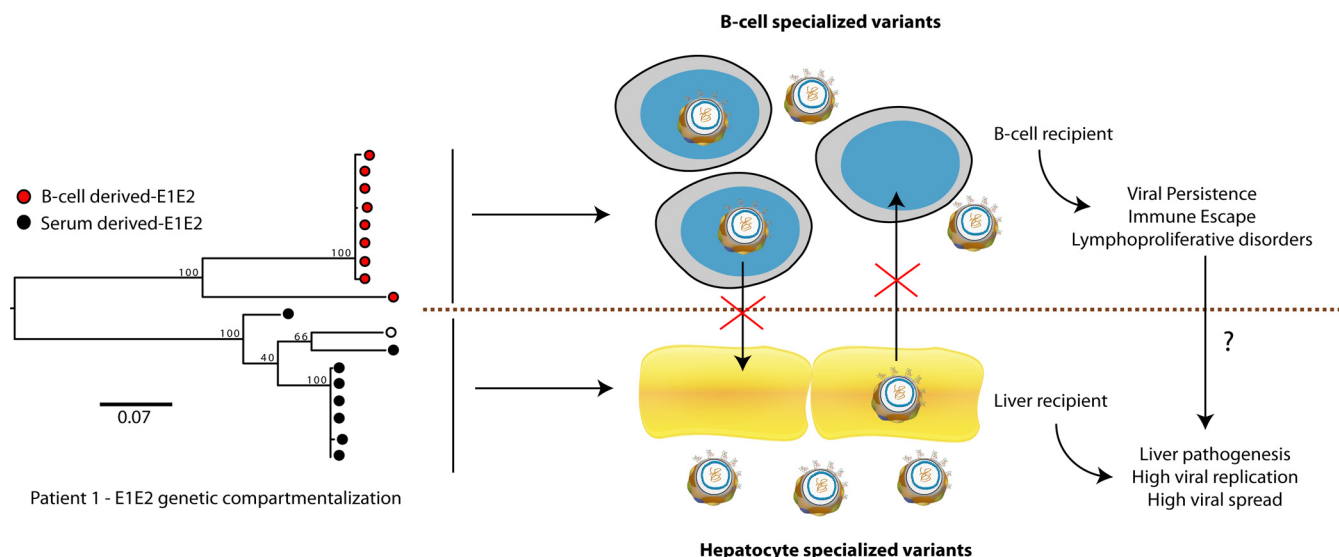


FIG 10 Potential genetic and clinical features of E1E2-dependent lymphotropism. The strong genetic compartmentalization observed between serum-derived E1E2 (black circle) and B-cell-derived E1E2 (red circle) suggests a strong specialization of these envelopes for hepatocytes and B cells, respectively. Accordingly, B-cell variants would infect and replicate specifically in B-cell compartments, whereas hepatocyte variants would replicate specifically within the liver. B-cell infection could then induce a viral persistence in HCV patients that undergo sustainable viral responses or liver transplantation. Such persistence could be associated with several extrahepatic manifestations as lymphoproliferative disorders. Dysfunction of B cells following infection may affect in return the immune response and contribute to enhance viral replication of liver-derived variants, and thus liver pathogenesis.

specific, E1E2-dependent process. In parallel, the incapacity of an anti-CD81 antibody to impair entry of HCV particles into B cells underlined that lymphotropic HCV variants might use alternative entry routes from CD81 to penetrate B cells. Such a hypothesis was strengthened by the observation that anti-CD81 antibody can slightly enhance the entry of L1a/JFH-1 virus into B cells. Consistently, previous reports have also demonstrated that the entry of patient-derived HCV particles into T cells depends on alternative cell surface molecules that are not involved in HCV entry into hepatocytes, such as the cell surface protein CD5 (21). In parallel, EWI-2wint is a cell surface molecule that has been shown to restrict HCV infection through the containment of CD81 into tetraspanin-enriched area (38). This molecule is expressed in several human non-liver cells such as B cells but not in hepatocytes, thus acting in the restricted hepatotropism of HCV. Hence, the ability of B-cell-specialized E1E2 to bypass such restriction when entering to B cells represents an additional argument that HCV lymphotropic strains might use alternative entry routes independent of CD81.

In the future, the characterization of such alternative routes could seriously improve our understanding of the molecular mechanisms governing HCV lymphotropism. In this regard, the HCVcc model represents a model of choice. Indeed, when incorporated onto HCVpp, the L1a and L3k E1E2 proteins presented a residual hepatotropism that contrasted with their very low hepatotropism when expressed onto HCVcc particles. By supporting proper viral particle assembly and virus-lipoprotein association, the HCVcc system likely represents a more relevant system than the HCVpp model to study HCV lymphotropism. A particular lipoprotein association, depending on unusual E1E2 conformations, could affect entry into hepatocytes and enhance B-lymphocyte infection. The presence of critical amino acid variants within the L1 E1E2 sequences could be responsible for such modified

interactions between HCV and lipoproteins and so far for the modification of HCV entry properties. Future studies aiming to isolate B-cell-derived full-length HCV genomes or HCV proteins involved in particle assembly will therefore be of strong interest to decipher particular interactions between the lipoprotein metabolism and HCV lymphotropic variants.

Patient 1 displayed two distinct genotypes (genotypes 1 and 2) that were specialized for hepatocytes and lymphocytes, respectively. It is interesting to point out that genotypes 1 and 2 are mainly found in patients with mixed cryoglobulinemia (MC) (39), suggesting that these two genotypes might also be the major mediators of HCV-related extrahepatic disorders. Two hypotheses can explain the presence of two distinct genotypes. First, patient 1 is a case of multiple infections, where both genotypes became highly specialized and predominant in the serum and in the lymphocytes. Second, lymphocyte specialization drove a high evolutionary rate of genotype 1 sequences that converged to the genotype 2 sequence type. The latter hypothesis is very unlikely given that they display very high divergence rates, and this would imply that these sequences converged toward an existing genotype. In the multiple-infection hypothesis, the competition between two genotypes would necessarily lead to the extinction of the less fit one over time, which is in accordance with the observation that cases of mixed infection in serum are very rare (40, 41). Therefore, the use of lymphocytes as hidden reservoirs could be a means for the less fit viruses to maintain their population and persist within an independent reservoir in a chronically infected patient (Fig. 10). Consequently, the strong specialization of some B-lymphocyte-derived variants is consistent with their inability to constitute a viral reservoir able to rapidly reinfect hepatocytes later after sustainable viral responses or liver transplantation (23, 42, 43) (Fig. 10). However, these variants likely constitute a significant source for viral persistence, lymphoproliferative disorders, and

immune escape. Dereglulation of PBMCs' immune functions could contribute in return to the maintenance of this viral persistence in lymphocytes, by promoting serum-derived variants' replication in liver tissues (Fig. 10). Therefore, understanding the dynamics and the diversity of HCV variants, their reservoirs, and their related genetic determinants may be essential to improve durable patient treatments.

ACKNOWLEDGMENTS

We are grateful to R. Bartenschlager, J. Dubuisson, H. Greenberg, K. Machida, C. Rice, and T. Wakita for providing reagents. Cytometry analyses were performed at the SFR BioSciences Gerland-Lyon Sud (US8/UMS 3444). We are grateful to our colleagues of the EVIR Team at CIRI, from UMR 5557 CNRS, and to members of UMR754 UCBL INRA EPHE for encouragement and advice.

This work was supported by the French Agence Nationale de la Recherche sur le Sida et les Hépatites Virales (ANRS) and by the European Research Council (ERC-2008-AdG-233130-HEPCENT). F.D., G.M., and L.-M.B. were supported by a fellowship from the French Ministry of Research (MESR).

FUNDING INFORMATION

EC | European Research Council (ERC) provided funding to François-Loïc Cosset under grant number ERC-2008-AdG-233130-HEPCENT. Agence Nationale de Recherches sur le Sida et les Hépatites Virales (ANRS) provided funding to Dimitri Lavillette under grant number AO2013.

REFERENCES

- Koike K. 2009. Steatosis, liver injury, and hepatocarcinogenesis in hepatitis C viral infection. *J Gastroenterol* 44(Suppl 19):S82–S88.
- Ferri C, Monti M, La Civita L, Longombardo G, Greco F, Pasero G, Gentilini P, Bombardieri S, Zignego AL. 1993. Infection of peripheral blood mononuclear cells by hepatitis C virus in mixed cryoglobulinemia. *Blood* 82:3701–3704.
- Zignego AL, Craxi A. 2008. Extrahepatic manifestations of hepatitis C virus infection. *Clin Liver Dis* 12:611–636, ix. <http://dx.doi.org/10.1016/j.cld.2008.03.012>.
- Blackard JT, Kemmer N, Sherman KE. 2006. Extrahepatic replication of HCV: insights into clinical manifestations and biological consequences. *Hepatology* 44:15–22. <http://dx.doi.org/10.1002/hep.21283>.
- Ploss A, Evans MJ. 2012. Hepatitis C virus host cell entry. *Curr Opin Virol* 2:14–19. <http://dx.doi.org/10.1016/j.coviro.2011.12.007>.
- Pileri P, Uematsu Y, Campagnoli S, Galli G, Falugi F, Petracca R, Weiner AJ, Houghton M, Rosa D, Grandi G, Abrignani S. 1998. Binding of hepatitis C virus to CD81. *Science* 282:938–941. <http://dx.doi.org/10.1126/science.282.5390.938>.
- Dao Thi VL, Granier C, Zeisel MB, Guerin M, Mancip J, Granio O, Penin F, Lavillette D, Bartenschlager R, Baumert TF, Cosset FL, Dreux M. 2012. Characterization of hepatitis C virus particle subpopulations reveals multiple usage of the scavenger receptor BI for entry steps. *J Biol Chem* 287:31242–31257. <http://dx.doi.org/10.1074/jbc.M112.365924>.
- Evans MJ, von Hahn T, Tschernie DM, Syder AJ, Panis M, Wolk B, Hatzioannou T, McKeating JA, Bieniasz PD, Rice CM. 2007. Claudin-1 is a hepatitis C virus co-receptor required for a late step in entry. *Nature* 446:801–805. <http://dx.doi.org/10.1038/nature05654>.
- Ploss A, Evans MJ, Gaysinskaya VA, Panis M, You H, de Jong YP, Rice CM. 2009. Human occludin is a hepatitis C virus entry factor required for infection of mouse cells. *Nature* 457:882–886. <http://dx.doi.org/10.1038/nature07684>.
- Pham TN, Michalak TI. 2008. Occult persistence and lymphotropism of hepatitis C virus infection. *World J Gastroenterol* 14:2789–2793. <http://dx.doi.org/10.3748/wjg.14.2789>.
- Blackard JT, Smeaton L, Hiasa Y, Horiike N, Onji M, Jamieson DJ, Rodriguez I, Mayer KH, Chung RT. 2005. Detection of hepatitis C virus (HCV) in serum and peripheral-blood mononuclear cells from HCV-monoinfected and HIV/HCV-coinfected persons. *J Infect Dis* 192:258–265. <http://dx.doi.org/10.1086/430949>.
- Durand T, Di Liberto G, Colman H, Cammas A, Boni S, Marcellin P, Cahour A, Vagner S, Feray C. 2010. Occult infection of peripheral B cells by hepatitis C variants which have low translational efficiency in cultured hepatocytes. *Gut* 59:934–942. <http://dx.doi.org/10.1136/gut.2009.192088>.
- Di Liberto G, Roque-Afonso AM, Kara R, Ducoulombier D, Fallot G, Samuel D, Feray C. 2006. Clinical and therapeutic implications of hepatitis C virus compartmentalization. *Gastroenterology* 131:76–84. <http://dx.doi.org/10.1053/j.gastro.2006.04.016>.
- Lerat H, Berby F, Trabaud MA, Vidalin O, Major M, Trepo C, Inchauspe G. 1996. Specific detection of hepatitis C virus minus strand RNA in hematopoietic cells. *J Clin Invest* 97:845–851. <http://dx.doi.org/10.1172/JCI118485>.
- Pal S, Sullivan DG, Kim S, Lai KK, Kae J, Cotler SJ, Carithers RL, Jr, Wood BL, Perkins JD, Gretch DR. 2006. Productive replication of hepatitis C virus in perihepatic lymph nodes in vivo: implications of HCV lymphotropism. *Gastroenterology* 130:1107–1116. <http://dx.doi.org/10.1053/j.gastro.2005.12.039>.
- Morsica G, Tambussi G, Sitia G, Novati R, Lazzarin A, Lopalco L, Mukenge S. 1999. Replication of hepatitis C virus in B lymphocytes (CD19+). *Blood* 94:1138–1139.
- Ducoulombier D, Roque-Afonso AM, Di Liberto G, Penin F, Kara R, Richard Y, Dussaix E, Feray C. 2004. Frequent compartmentalization of hepatitis C virus variants in circulating B cells and monocytes. *Hepatology* 39:817–825. <http://dx.doi.org/10.1002/hep.20087>.
- Roque-Afonso AM, Ducoulombier D, Di Liberto G, Kara R, Gigou M, Dussaix E, Samuel D, Feray C. 2005. Compartmentalization of hepatitis C virus genotypes between plasma and peripheral blood mononuclear cells. *J Virol* 79:6349–6357. <http://dx.doi.org/10.1128/JVI.79.10.6349-6357.2005>.
- Mizutani T, Kato N, Ikeda M, Sugiyama K, Shimotohno K. 1996. Long-term human T-cell culture system supporting hepatitis C virus replication. *Biochem Biophys Res Commun* 227:822–826. <http://dx.doi.org/10.1006/bbrc.1996.1591>.
- Mizutani T, Kato N, Saito S, Ikeda M, Sugiyama K, Shimotohno K. 1996. Characterization of hepatitis C virus replication in cloned cells obtained from a human T-cell leukemia virus type 1-infected cell line, MT-2. *J Virol* 70:7219–7223.
- Sarhan MA, Pham TN, Chen AY, Michalak TI. 2012. Hepatitis C virus infection of human T lymphocytes is mediated by CD5. *J Virol* 86:3723–3735. <http://dx.doi.org/10.1128/JVI.06956-11>.
- Sung VM, Shimodaira S, Dougherty AL, Picchio GR, Can H, Yen TS, Lindsay KL, Levine AM, Lai MM. 2003. Establishment of B-cell lymphoma cell lines persistently infected with hepatitis C virus in vivo and in vitro: the apoptotic effects of virus infection. *J Virol* 77:2134–2146. <http://dx.doi.org/10.1128/JVI.77.3.2134-2146.2003>.
- Schramm F, Soulier E, Royer C, Weitten T, Fafi-Kremer S, Brignon N, Meyer N, Ellero B, Woehl-Jaegle ML, Meyer C, Wolf P, Doffoel M, Baumert TF, Stoll-Keller F, Schvoerer E. 2008. Frequent compartmentalization of hepatitis C virus with leukocyte-related amino acids in the setting of liver transplantation. *J Infect Dis* 198:1656–1666. <http://dx.doi.org/10.1086/592986>.
- Sarhan MA, Chen AY, Russell RS, Michalak TI. 2012. Patient-derived hepatitis C virus and JFH-1 clones differ in their ability to infect human hepatoma cells and lymphocytes. *J Gen Virol* 93:2399–2407. <http://dx.doi.org/10.1099/vir.0.045393-0>.
- Marukian S, Jones CT, Andrus L, Evans MJ, Ritola KD, Charles ED, Rice CM, Dustin LB. 2008. Cell culture-produced hepatitis C virus does not infect peripheral blood mononuclear cells. *Hepatology* 48:1843–1850. <http://dx.doi.org/10.1002/hep.22550>.
- Flint M, Thomas JM, Maidens CM, Shotton C, Levy S, Barclay WS, McKeating JA. 1999. Functional analysis of cell surface-expressed hepatitis C virus E2 glycoprotein. *J Virol* 73:6782–6790.
- Flint M, Maidens C, Loomis-Price LD, Shotton C, Dubuisson J, Monk P, Higginbottom A, Levy S, McKeating JA. 1999. Characterization of hepatitis C virus E2 glycoprotein interaction with a putative cellular receptor, CD81. *J Virol* 73:6235–6244.
- Lindenbach BD, Evans MJ, Syder AJ, Wolk B, Tellinghuisen TL, Liu CC, Maruyama T, Hynes RO, Burton DR, McKeating JA, Rice CM. 2005. Complete replication of hepatitis C virus in cell culture. *Science* 309:623–626. <http://dx.doi.org/10.1126/science.1114016>.
- Douam F, Dao Thi VL, Maurin G, Fresquet J, Mompelat D, Zeisel MB, Baumert TF, Cosset FL, Lavillette D. 2014. Critical interaction between E1 and E2 glycoproteins determines binding and fusion properties of hepatitis C virus during cell entry. *Hepatology* 59:776–788. <http://dx.doi.org/10.1002/hep.26733>.

30. Bartosch B, Dubuisson J, Cosset FL. 2003. Infectious hepatitis C virus pseudo-particles containing functional E1-E2 envelope protein complexes. *J Exp Med* 197:633–642. <http://dx.doi.org/10.1084/jem.20021756>.
31. Edgar RC. 2004. MUSCLE: multiple sequence alignment with high accuracy and high throughput. *Nucleic Acids Res* 32:1792–1797. <http://dx.doi.org/10.1093/nar/gkh340>.
32. Criscuolo A, Gribaldo S. 2010. BMGE (Block Mapping and Gathering with Entropy): a new software for selection of phylogenetic informative regions from multiple sequence alignments. *BMC Evol Biol* 10:210. <http://dx.doi.org/10.1186/1471-2148-10-210>.
33. Guindon S, Gascuel O. 2003. A simple, fast, and accurate algorithm to estimate large phylogenies by maximum likelihood. *Syst Biol* 52:696–704. <http://dx.doi.org/10.1080/10635150390235520>.
34. Tarr AW, Owsianka AM, Szwejk A, Ball JK, Patel AH. 2007. Cloning, expression, and functional analysis of patient-derived hepatitis C virus glycoproteins. *Methods Mol Biol* 379:177–197. http://dx.doi.org/10.1007/978-1-59745-393-6_13.
35. Blanchard E, Belouzard S, Goueslain L, Wakita T, Dubuisson J, Wychowski C, Rouille Y. 2006. Hepatitis C virus entry depends on clathrin-mediated endocytosis. *J Virol* 80:6964–6972. <http://dx.doi.org/10.1128/JVI.00024-06>.
36. Meuleman P, Hesselgesser J, Paulson M, Vanwolleghem T, Desolliere I, Reiser I, Leroux-Roels G. 2008. Anti-CD81 antibodies can prevent a hepatitis C virus infection in vivo. *Hepatology* 48:1761–1768. <http://dx.doi.org/10.1002/hep.22547>.
37. Jopling CL, Yi M, Lancaster AM, Lemon SM, Sarnow P. 2005. Modulation of hepatitis C virus RNA abundance by a liver-specific microRNA. *Science* 309:1577–1581. <http://dx.doi.org/10.1126/science.1113329>.
38. Potel J, Rassam P, Montpellier C, Kaestner L, Werkmeister E, Tews BA, Couturier C, Popescu CI, Baumert TF, Rubinstein E, Dubuisson J, Milhiet PE, Cocquerel L. 2013. EWI-2wint promotes CD81 clustering that abrogates hepatitis C virus entry. *Cell Microbiol* 15:1234–1252. <http://dx.doi.org/10.1111/cmi.12112>.
39. Nguyen QT, Leruez-Ville M, Ferriere F, Cohen P, Roulot-Marullo D, Coste T, Deny P, Guillemin L. 1998. Hepatitis C virus genotypes implicated in mixed cryoglobulinemia. *J Med Virol* 54:20–25. [http://dx.doi.org/10.1002/\(SICI\)1096-9071\(199801\)54:1<20::AID-JMV4>3.0.CO;2-R](http://dx.doi.org/10.1002/(SICI)1096-9071(199801)54:1<20::AID-JMV4>3.0.CO;2-R).
40. Viazov S, Widell A, Nordenfelt E. 2000. Mixed infection with two types of hepatitis C virus is probably a rare event. *Infection* 28:21–25. <http://dx.doi.org/10.1007/s150100050005>.
41. Antonishyn NA, Ast VM, McDonald RR, Chaudhary RK, Lin L, Andonov AP, Horsman GB. 2005. Rapid genotyping of hepatitis C virus by primer-specific extension analysis. *J Clin Microbiol* 43:5158–5163. <http://dx.doi.org/10.1128/JCM.43.10.5158-5163.2005>.
42. Di Liberto G, Feray C. 2005. The anhepatic phase of liver transplantation as a model for measuring the extra-hepatic replication of hepatitis C virus. *J Hepatol* 42:441–443. <http://dx.doi.org/10.1016/j.jhep.2005.02.001>.
43. Gray RR, Strickland SL, Veras NM, Goodenow MM, Pybus OG, Lemon SM, Fried MW, Nelson DR, Salemi M. 2012. Unexpected maintenance of hepatitis C viral diversity following liver transplantation. *J Virol* 86:8432–8439. <http://dx.doi.org/10.1128/JVI.00749-12>.